HAWASSA UNIVERSITY

INSTITUTE OF TECHNOLOGY

FACULTY OF ELECTRICAL AND COMPUTER ENGINEERING

OPTIMAL PLACEMENT AND SIZING OF UNIFIED POWER FLOW CONTROLLER (UPFC) FOR VOLTAGE STABILITY ENHANCEMENT: CASE GERD TO HOLETA 500/400 KV TRANSMISSION LINE NETWORK.

A THESIS SUBMITTED

IN PARTIAL FULFILLMENT OF THE REQUIREMENTS FOR THE DEGREE OF MASTER OF SCIENCE IN POWER SYSTEM AND ENERGY ENGINEERING

BY

GETAHUN SISAY

HAWASSA, ETHIOPIA

March 2025

OPTIMAL PLACEMENT AND SIZING OF UNIFIED POWER FLOW CONTROLLER (UPFC) FOR VOLTAGE STABILITY ENHANCEMENT

(CASE STUDY: GERD TO HOLETA 500/400 KV TRANSMISSION LINE NETWORK)

By: GETAHUN SISAY

ADVISOR: SOLOMON MAMO (PHD)

CO-ADVISOR: Mr. TESFAHUN MOLA (MSc)

A THESIS SUBMITTED TO DEPARTEMENT OF ELECTRICAL AND COMPUTER ENGINEERING

HAWASSA INSTITUTE OF TECHNOLOGY, SCHOOL OF GRADUATE STUDIES

HAWASSA UNIVERSITY, HAWASSA, ETHIOPIA

IN PARTIAL FULFILLMENT OF THE REQUIREMENTS FOR THE DEGREE OF MASTERS OF SCIENCE IN POWER SYSTEM AND ENERGY ENGINEERING

MARCH, 2025

OPTIMAL PLACEMENT AND SIZING OF UNIFIED POWER FLOW CONTROLLER (UPFC) FOR VOLTAGE STABILITY ENHANCEMENT:
CASE GERD TO HOLETA 500/400 KV TRANSMISSION LINE NETWORK.

BY

GETAHUN SISAY

Thesis Submitted to Hawassa University, Institute of Technology, Department of Electrical and Computer Engineering, for the Partial Fulfillment of the Requirement for the Degree of Masters of Science in Power System and Energy Engineering.

Advisor: Dr. Solomon Mamo

Co-Advisor: Mr.Tesfahun Mola

HAWASSA, ETHIOPIA

March 2025

HAWASSA UNIVERSITY

INSTITUTE OF TECHNOLOGY

SCHOOL OF RESEARCH AND POSTGRADUATE STUDIES

FACULTY OF ELECTRICAL AND COMPUTER ENGINEERING

ADVISOR'S APPROVAL SHEET

THIS IS TO CERTIFY THAT THE THESIS ENTITLED

Optimal Placement and Sizing of Unified Power Flow Controller (UPFC) for Voltage Stability Enhancement: Case of GERD to Holeta 500/400 KV Transmission Line Network
This thesis is submitted in partial fulfillment of the requirements for the degree of Master of Science in Electrical Engineering, specializing in Power System and Energy Engineering, within the Graduate Program of the Department of Electrical and Computer Engineering. The research was conducted by **Getahun Sisay** under my supervision. Based on the completion of this work, I recommend that the student has fulfilled the necessary requirements and should proceed with submitting the thesis to the department.

Dr. Solomon M	____ ____	__**28/02/2025**___
Advisor	signature	Date
Mr.Tesfahun Mola	__________	__________
Co-Advisor	signature	Date

Declaration

I, Getahun Sisay, hereby declare that this thesis, entitled **"Optimal Placement and Sizing of Unified Power Flow Controller (UPFC) for Voltage Stability Enhancement: Case of GERD to Holeta Transmission Line Network,"** is my original work. The work presented in this thesis has not been submitted previously for the fulfillment of a degree at this or any other university. All sources and materials used in the thesis have been properly acknowledged.

GETAHUN SISAY ________________________ ___________________

This thesis is submitted for examination with my approval as university advisor

Dr. Solomon Mamo	_________	__________
Main Advisor	signature	Date
Mr. Tesfahun Mola	_________	_________
Co-Advisor	signature	Date

HAWASSA UNIVERSITY

SCHOOL OF RESEARCH AND POSTGRADUATE STUDIES

EXAMINER'S APPROVAL SHEET

We, the undersigned members of the Board of Examiners for the final open defense of **Getahun Sisay**, have read and evaluated his thesis titled **"Optimal Placement and Sizing of Unified Power Flow Controller (UPFC) for Voltage Stability Enhancement : Case of GERD to Holeta Transmission Line Network"** and have examined the candidate.

Therefore, we certify that the thesis has been accepted in partial fulfillment of the requirements for the Master's degree.

Dr Solomon Mamo ____________ ______________

Main Advisor signature Date

Dr Yeshitila Shiferawu ____ ___ **08/04/2025**

External Examiner signature Date

Dr Teshome Lindi ____________ ______________

Internal Examiner signature Date

Mr. Tesfaye Hailu ___________ ______________

Chair holder signature Date

Mr.Dejene Hurissa ____________ ______________

Faculty Dean Signature Date

Final approval and acceptance of the thesis is contingent upon the submission of the final copy of the thesis to the school of graduate studies (SGS) through the department Graduate Committee (DGC) of Electrical and Computer Engineering.

Acknowledgment

First and foremost, I would like to express my heartfelt thanks and praise to the Omnipotent, Omnipresent, and Omniscient Almighty God. Next, I am deeply grateful to my advisors, Dr. Solomon Mamo and MrTesfahun Mola. For their invaluable guidance, timely feedback, and unwavering commitment. I truly appreciate their motivation and support throughout this journey. I would also like to extend my sincere thanks to all the engineers at the Ethiopian Electric Power (EEP), for their generous assistance in providing the information and data necessary for this work. Finally, I am forever thankful to my beloved family for their constant encouragement and support, which helped me stay, focused and motivated throughout my studies. I also want to express my appreciation to all my dear friends who offered their support and contributed to the completion of this thesis.

Abstract

The GERD to HOLETA 500/400 KV transmission line network was assessed to determine the optimal location and size for a Unified Power Flow Controller (UPFC) to enhance voltage stability. Due to the long transmission path and rising load demand, system components have become overloaded, causing power outages. To evaluate the current power system conditions, the Newton-Raphson load flow technique was used in the power flow model. The voltage stability index shows signs of instability, and load flow analysis reveals that all bus voltages, except for the slack bus, fall outside the acceptable range. Active and reactive power losses on the transmission line are 0.491 MW and 0.4689 MVAR, respectively; while the systems rated capacity is 2591 MW and 1255 MVAR. The minimum required voltage is 0.95 pu, but the actual minimum voltage magnitude and stability are 0.872 pu and 0.5262 pu, respectively. UPFCs, as reactive power compensation devices, are proven to enhance voltage stability, power losses, and voltage profiles. The UPFC was sized and placed using Grey Wolf Optimization (GWO) to minimize power losses, improve voltage stability, and optimize the voltage profile. The optimal UPFC size is 757.5 KVAR, and the best location is bus 3. With UPFC compensation, the bus's minimum voltage magnitude and stability improve to 0.9668 pu and 0.83477 pu, respectively, while active and reactive power losses decrease to 0.1655 MW and 0.03302 MVAR. After implementing UPFC compensation, the annual energy loss cost is reduced from 10.343 million Birr to3 .486million Birr, and the total cost of a 757.5 KVAR, UPFC is 5.708 million birr including installation cost for resulting in a savings of 1.142 million Birr and a payback period of 12 months. The economic analysis confirms the solution is both effective and cost-efficient.

Key Words: - Unified power flow controller, Grey Wolf Optimization, Voltage profile enhancement, voltage stability, Power loss

Contents

List of Table

List of figure

Acronym

ATC	Available Transfer Capability
AC	Alternating current
EMTP	Electromagnetic Transients Program
FACTS	Flexible Alternating Current Transmission Line
PST	Phase shifting transformer
STATCOM	Static Condenser
TCSC	Thyristor Controlled Series Capacitor
TCPR	Thyrisistor controlled Phase angle Regulator
SVC	Static VAR compensator
VSC	Voltage sourced converters
SSSC	Static synchronous series compensator
SPWM	Sinusoid pulse width modulation
GWO	Grey Wolf optimization

CHAPTER ONE

1.1 Introduction

The most intricate and costly man-made system is the power system, which includes the generation, transmission, and distribution of electric energy. Since the inception of modern civilization, power systems have been a critical component of human daily life, particularly in the industrial and economic sectors. The development of any contemporary nation is significantly influenced by the energy, electricity that is generated by power systems [1]. The voltage stability of the power system will be adversely affected by the environmental constraints that restrict the expansion of transmission networks and generation in close proximity to demand centers. Consequently, the voltage stability limit has impacted power systems due to the high demand for electrical power and the lack of a concurrent increase in transmission capacity [2]. The power systems are inherently complex in terms of generation, transmission, and distribution. Consequently, it is necessary to carefully design and implement the devices to mitigate stability-related issues and to control the power flow, particularly in the transmission system, in order to be able to adapt to any momentary system conditions. The operation of AC power transmission lines, which are typically restricted by network parameters and operating variables, is facilitated by the use of FACTS technology, including STATCON (Static Condenser), Thyristor Controlled Series Capacitor (TCSC), Thyrisistor controlled Phase angle Regulator (TCPR), and UPFC. It is important to quickly and flexibly manage network parameters including bus voltages, line impedances, and phase shift angles in the power system. Instead of selecting a specific controller, FACTS show the range of controllers from which the system designer can select based on cost-benefit analysis. In contemporary power systems, the placement of the UPFC is crucial in resolving the majority of power flow control problems. In the current power system industry, UPFC is responsible for controlling voltage, line impedance, and phase angles in order to improve power security, lower generation costs, and increase power transfer capabilities. Moreover, UPFC handles load sharing across parallel corridors, power flow management, and loop flow control [3]. Adequate Available Transfer Capability (ATC) is necessary for free access to transmission networks in a deregulated environment in order to ensure economic transactions. In any case, there has always been the possibility of building new transmission lines, but social issues and environmental constraints should be taken into account. In actuality, building new transmission lines is highly costly and unprofitable for network industry owners. Therefore, it is preferable and advised that many power systems sectors worldwide accept the efficient use of the current transmission networks with the assistance of new gadgets [4]. Instantaneously, FACTS controllers are used to respond to stability issues, improve or decrease power flow in designated lines, and govern the transmission of alternating current (AC). The ability to regulate the path of power flow, connect under-connected networks, and enable energy exchange between distant agents are the ultimate potential of this technology (FACT). Using FACTS devices, which are power electronic-based devices, facilitates power transfer capability and controllability. Based on their switching technology, these devices can be divided into three categories: fast switched, utilizing IGBTs, or mechanically switched thyristor switched. New advancements in power electronics, such as phase shifting transformers (PST) and static VAR compensators (SVC) in power systems have expanded the variety of applications for FACTS. Furthermore, the flexibility and controllability of FACTS also help to mitigate concerns related to the intermittent renewable energy sources, increase international power flow, and mitigate the unreliable supply challenges of the renewable. Standard wind farms are unable to deliver SVC and STATCOM's fault-resolution capabilities and auxiliary services (such as voltage management) to the grid [5].

The solid-state synchronous voltage sources (SVSs), first proposed by L. Gyugyi in the late 1980s, and are the foundation of the most recent generation of FACTS controllers. The SVS functions as an ideal synchronous machine, producing fundamental frequency three-phase balanced sinusoidal voltages with controllable amplitude and phase angle. Reactive power can be generated internally by both capacitive and inductive means. Voltage-sourced converters (VSC) can be used to design and implement the SVS, which can be utilized as a series or shunt compensator. It is known as a static condenser (STATCON) if it functions as a reactive shunt compensator, static synchronous series compensator (SSSC) if it functions as a reactive series compensator. The Unified Power Flow Controller (UPFC) is a configuration of two SVSs, one connected in series with the ac system and the other connected in shunt, with common dc terminals [6].

1.2 Statement of the Problem

Instability issues have been identified within the power system, particularly in the transmission line network [12]. The system fails to maintain proper stability during both normal and overloaded conditions. These issues stem from system malfunctions and fluctuations in load demand. A significant portion of the power generated at the GERD power plant is transmitted to the HOLETA 500/400 kV bus bar, where voltage deviations are also observed. The transmission line faces both active and reactive power losses, and voltage levels at most bus bars fall below 95%, indicating poor voltage regulation. This situation leads to increased real and reactive power losses along the transmission line and, consequently, substantial power losses, which contribute to voltage instability. To address this, deploying Flexible AC Transmission System (FACTS) devices, specifically a Unified Power Flow Controller (UPFC), is an optimal solution. This would help compensate for reactive power and improve the voltage profile to comply with IEEE and ICE standards of $0.95 \leq Vi \leq 1.05$ pu, which also align with Ethiopian Electric Power and Utility regulations. Furthermore, this solution would reduce power losses at the HOLETA 500/400 kV bus bars by over 4.4%. Notably, except for the slack bus, the voltage profile at all other bus bars remains below the required 95% threshold, as per IEEE and ICE standards ($0.95 \leq Vi \leq 1.05$ pu).

1.3 Objectives of the Study

1.3.1 General Objective

The Main objective of this thesis is to determine the optimal placement and sizing of Unified Power Flow (UPFC) in the GERD to Holeta transmission line network to enhance Voltage stability and power system performance using Grey Wolf Optimization method.

1.3.2 Specific Objectives

- ✓ To identify the optimal placement and sizing of UPFC in Transmission network Using Grey Wolf Optimization Method.
- ✓ To model GERD to HOLETA transmission line network with UPFC using MATLAB Simulink software.
- ✓ Analysis the power system voltage stability index profile and voltage profile of GERD to Holeta transmission line network with and without UPFC devices.
- ✓ To compare the results of system performance with and without UPFC.

1.4 Significance of the Study

When a problem occurs in the power transmission system, both suppliers and customers are simultaneously affected. This thesis is highly significant for both the utility and customer sides. Some of its key benefits include:

- Increased power transfer capability, allowing for additional load.
- Reduced costs by eliminating the need for new distribution networks.
- Identification of areas where major improvements are required.
- Improved product quality, enhanced industry benefits, and increased customer satisfaction.

FACTS devices, especially UPFC, have emerged as an innovative solution to address these power system challenges by managing various system variables simultaneously and independently. However, there is limited research on the use of FACTS devices, particularly UPFC. This research aims to meet the growing demand for efficient power system utilization, both in Ethiopia and globally. Furthermore, it will provide a level of assurance regarding the security and effectiveness of UPFC FACTS devices [13].

1.5 Organization

This study is organized into five chapters. Chapter 1 introduces the research, covering the problem statement, objectives, and significance of the study. Chapter 2 focuses on the literature review, addressing existing research and identifying gaps. It also provides a brief overview of power system challenges, FACTS devices and their classifications, as well as their benefits. Additionally, the chapter discusses recent developments in power electronics, particularly regarding the Unified Power Flow Controller (UPFC). Chapter 3 presents the mathematical modeling of UPFC devices for power flow analysis in power systems, including a comparison of their steady-state performance. Chapter 4 offers an analysis of the research findings, and Chapter 5 concludes the study with suggestions and recommendations for future work.

CHAPTER TWO

2.1 LITERATURE REVIEW

In order to supply customers with electricity, the transmission system connects the distribution system and the power generation. The ultimate goal of a power system is to reliably and economically deliver electricity to consumers. Numerous scholars have put up various approaches to address the issue of transmission system optimization, as well as techniques for enhancing and stabilizing voltage profiles. Researchers have recently been leaning toward the unified power flow controller (UPFC) as a way to improve the system and increase voltage stability. Using various methods and taking into account various goals, a lot of work has recently been put into solving the optimal unified power flow controller (UPFC) placement and sizing problem and they proposed their best solution to the existing problems. A few of them are mentioned below: This thesis focused on UPFC modeling and control, with the ultimate goal of offering practical techniques and instruments for evaluating UPFC's influence on transmission system reinforcement. The accompanying models, algorithms, and control strategies of UPFC have been thoroughly reviewed in the thesis, which breaks down the modeling and control of UPFC into a number of smaller issues. The UPFC's intricate power electronic gadget and internal closed-loop controller have been used to put up an electromagnetic transient prototype model. It has been detailed how EMTP handles the issues that arise during the process of creating such a model. The implementation of this EMTP-based simulator of SPWM UPFC has been a helpful tool in supporting the creation and validation of a more thorough and functional model of the UPFC for future research [1].

In order to increase the power system's voltage stability, this paper discusses the best site for UPFC based on the Firefly algorithm. The enhanced searching capability, random reduction, and decreased complexity were examples of the innovative aspects of the suggested approach. In this sense, the generator outage increases power loss and impacts the system voltage stability limitations. Additionally, the FA method determines the best placement for the UPFC by optimizing the highest power loss line [2]. Recent advancements in power electrical and computing control technology can provide greater flexibility in managing power flow in contemporary power systems. The three system variables—line reactance, magnitude, and phase angle difference of voltage across the line—can all be controlled by the Unified Power Flow Controller (UPFC), a Flexible AC transmission system (FACTS) device. In contemporary power systems, the UPFC offers a potential way to regulate power flow. Effective control setting, which may be achieved with a power flow analysis tool, is essentially, what determines performance. According to these investigations, the approach preserves the fundamental NRLF characteristics, including a high degree of precision, a quick computing time, and a good rate of convergence [3]. This study examines how the power system is affected by the Unified Power Flow Controller's (UPFC) location. This study examines multiple case studies that include different locations for UPFC installation on the power system and obtains the voltage profile at each system bus. After UPFC is installed at different points throughout the power system, the active and reactive of all transmission lines is examined, and the findings are evaluated. Congestion in the power system is largely caused by the promotion of HV line building, the quantity of power transmission/km on HV lines, and the amount of power transactions as perceived from an economic perspective. The employment of FACTS devices, particularly UPFC, is the answer. This study examines UPFC and the different potential locations for its installation on the power system. Second, the control system's operation in its converters is also examined. Finally, its usage as a power flow controller and voltage injection is demonstrated by placing UPFC in a transmission link and modeling a power system using MATLAB/SIMULINK. Conclusions are drawn from various findings to demonstrate the advantages of UPFC in the power system [4]. This thesis focused on the Unified Power Flow Controller (UPFC), a FACTS device. This device has a significant impact on power system stability because to its exceptional capacity to concurrently control actual and reactive power flows on a transmission line and to regulate voltage at the bus to which it is connected. Knowing that the UPFC can permit loading of the transmission lines near their thermal limitations, pushing the power to flow through the intended pathways, makes these aspects even more important. This will provide much-needed flexibility to power system operators to meet the demands of the deregulated power system [6]. One of the main areas of study in this research project is the upkeep and dependability of the power system, particularly the transmission line. Congestion in the power system is largely caused by the promotion of HV line building, the quantity of power transmitted per kilometer on HV lines, and the amount of power transactions as perceived from an economic perspective. The application of FACTS devices, particularly UPFC, is taken into consideration as a remedy. The investigation of UPFC and its many modes of operation were comprehended in this study. Second, the way its converters' control system operated was also examined. Ultimately, its application as a power flow controller and voltage injection was demonstrated through the use of MATLAB to model a power system and the installation of UPFC in a transmission link. Conclusions were drawn from several findings to demonstrate the advantages of UPFC in the power system [5]. The Static Synchronous Compensator (STATCOM) and the Unified Power Flow Controller (UPFC), two Flexible AC Transmission System (FACTS) devices for controlling voltage and power flow in transmission systems, respectively, are also examined in this thesis. These results in a quicker reaction than with conventional equipment made up of mechanically based or switched components. As a result, power flow can be controlled more freely, and transmission cables can be safely loaded to levels closer to their thermal limitations. The behavior of these devices during faults in the transmission system is also presented [7]. In order to regulate power flow in the transmission line, the Unified Power Flow Controller may regulate power system characteristics such as voltage, line reactance, and phase angle. A suitable voltage with a phase angle is injected into the transmission line to control the flow of power. This study uses a typical PI controller to create a decoupled control system for shunt and series converters in order to track the reference power inputs. Software called MATLAB/SIMULINK was used for modeling. The system under various load circumstances and power factors was analyzed. The findings demonstrate that UPFC can monitor power variations and provide an appropriate voltage to the power system to sustain power flow [8]. The power flow in the transmission networks was managed by the Unified Power Flow Controller (UPFC), which controlled the phase angle, voltage magnitude, and impedance. The power system benefits from this controller in terms of both static and dynamic operation. Additionally, it introduces fresh difficulties in the design of power systems and power electronics. The two voltage source inverters (VSI) that make up the UPFC's basic structure are linked in series with the transmission line (SSSC) and parallel to the transmission line (STATCOM). The theoretical description of the UPFC system, its modeling, and a case study using Matlab/Simulink simulation are presented in this paper. The paper's objectives are to model, identify references, control, and examine the effects of UPFC on the electrical network. Lastly, the results of the simulation have been shown to show that the UPFC's ability to regulate voltage in power systems has improved [9]. Investigating how the SVCs in the HOLETA 500/400kV substation affect voltage stability and power transfer enhancement was the main goal of this research. At the HOLETA 500/400 kV substation, three SVCs with a combined capacity of 900 MVAr are in use. They use 400/33 kV coupling transformers to connect to the AC 400 kV system. Additionally, the study assessed the potential installation (location) of SVCs at the DEESA or GERD substation and examined the impact on transferred power and voltage stability. The MATLAB 2017a/Simulink environment was used to simulate the system in this investigation [10].

Table2.1 literature review summary

No	Author Name	Title	Advantage	Method (optimization)	Disadvantage
1	Jun Yong Liu	Modelling and control of unified power flow for reinforcement of transmission systems.	The effectiveness of the proposed algorithm has been compared with the user defined model method	power injection model based control method (PIM)	Internal controllers, PID is not such accurate.
2	MOHAMED JALBOUB	Investigation of the Application of UPFC Controllers for Weak Bus Systems Subjected to Fault Conditions	Validation is made on IEEE 14 bus system.	Firefly algorithm based optimal	The comparison of cost analysis does not done.
3	Sunil Kumar Jilledi	Implementing of UPFC in the Power System Network to Control Power Flow and Minimization of Losses	Power flow between the lines is improved to a pre specified value.	Newton-Raphson Load Flow	Control method is not mentioned.
4	Abebaw Yalew Mengistu	study on power transfer capability and voltage stability improvement using	Detailed models of the SVCs are implemented and tested.	MATLAB/ Simulink Sims cape.	Optimization method to install SVC is not considered and

		static var compensator			cost analysis is not made.

2.2 Research Gap

The Grey Wolf Optimization (GWO) algorithm, a relatively new approach for power system optimization, has shown promising results in solving complex power system issues, especially in terms of optimal placement. However, a significant portion of the existing literature has not applied the GWO method to address these problems.

2.3 Functional structure of power system

In real case, power systems operate at various levels of voltage levels which are separated by transformers. Based on voltage-level, a power transmission system network can be categorized into the following subsystems.

a) Transmission system
b) Sub transmission system
c) Distribution system

a) All major generation stations as well as main load centers in the system are interconnected by the transmission system. It operates with the highest voltage level and handles a large amount of power. Through tie lines, power can be transported from one power system to other power systems that belong to the same power pool.

b) The sub-transmission system acts as an intermediary between the transmission and distribution systems, transmitting smaller amounts of power from transmission substations to distribution substations. In some cases, however, large industrial customers are directly served by the sub-transmission system. Typically, the voltage in this system ranges from 11 kV to 132 kV.

c) The final stage of power delivery to customers is through the distribution system. Primary distribution voltages generally range from 4 kV to 34.5 kV, with small industrial customers being supplied via primary feeders at this voltage level. Modern power systems are made up of multiple generation sources and various layers of transmission and distribution networks. This structure provides a high degree of redundancy, allowing the system to withstand unusual contingencies without causing service disruptions. However, as power systems expand, they grow into vast, complex networks. Consequently, the design and secure operation of such a system become increasingly challenging a challenging problem [1].

2.4 FACTS Devices, Classification and Reactive power compensation techniques

Reactive power compensation plays a crucial role in minimizing power loss, improving the power factor, and enhancing the voltage stability index of a power system. As the reliability and quality of electrical power become increasingly important, reactive power compensation is a key strategy for ensuring dependable and high-quality power systems. Various technologies are employed for reactive power compensation, including synchronous condensers, static VAR compensators, capacitor banks, series compensators, and shunt reactors. These technologies are compared to identify the best reactive power sources, and optimization methods, such as D-STATCOM, are applied to enhance performance. Based on observations and analysis, the most effective technology and optimization strategies are recommended for future projects [4].

Custom power devices such as the Distribution Static Compensator (D-STATCOM), Dynamic Voltage Restorer (DVR), Unified Power Quality Conditioner (UPQC), and Battery Energy Storage System (BESS) are essential tools for improving power quality. These devices are particularly useful for addressing power quality issues, though their high cost requires careful placement within the system to maximize their effectiveness. Some of the advantages of compensating devices include active filtering, load balancing, power factor correction, and voltage regulation. While D-STATCOM is commonly used in radial distribution systems, it shares structural and functional similarities with the STATCOM used in transmission systems [14]. D-STATCOM and the power system are connected in a shunt configuration, while a Dynamic Voltage Restorer (DVR) operates in series, injecting series voltage to adjust the supply voltage. However, injecting a large amount of voltage into the system can lead to a cascade voltage failure, requiring a sophisticated control system. The structure of the Unified Power Quality Conditioner (UPQC) is similar to that of the Unified Power Flow Controller (UPFC), as it introduces both shunt currents and series voltage into the system.

In distribution networks, reactive power compensation techniques are employed to improve power quality and reduce losses. Reactive power is the power transferred between the distribution system and loads that include inductive or capacitive components. Ideally, reactive power would be zero in a power system, but due to the presence of inductive and capacitive loads, it is unavoidable in practice. These techniques are essential for enhancing power quality and minimizing losses. One common method for reactive power correction in distribution networks is through the use of voltage source converters, often known as FACTS controllers. These controllers regulate power flow, improve power transfer capacity, reduce costs, and enhance the stability and security of power systems [4]. To improve the operation of large-scale electrical networks in today's power sector, reactive power regulation techniques such as controlled shunt reactors in extra-high-voltage transmission lines must be implemented [2]. FACTS (Flexible AC Transmission Systems) are advanced transmission systems that use high-power electronics to increase their capacity and controllability. Custom Power refers to the application of power electronics in utility distribution networks, tailored to meet the specific needs of commercial and industrial users. These technologies are developed to overcome the limitations of traditional, mechanically controlled AC transmission systems. The power electronic controllers mentioned above offer the following key benefits to the power sector:

Allow flows of power on the prescribed transmission routes.

a) By avoiding overloading they secure loading of transmission lines to their thermal limits.
b) Reduce generation margins of cost by enhancing transmission capacity (rather than construction of new generation as well as distribution system).
c) Prevent cascading outages by limiting the impact of faults and equipment failure.

2.4.1 Dynamic Voltage Restorer

It can be thought of as a variable or controllable voltage source that is coupled in series with the load (VL) and the point of common coupling (PCC). By injecting the proper voltage during voltage quality events, the DVR regulates the load voltage profile and controls the interchange of actual and reactive power between the DVR and the distribution system. Features like series conditioning, harmonic compensation, and sub-cycle protection can enhance the DVR's value and raise demand for it in industries with important clients. Additionally, DVR prevents load tripping under sag situations. With DVR, the micro grid's low-voltage ride-through capacity can be enhanced. The DVR employs the same blocks as the D-STATCOM, but in this application, the coupling transformer is connected in series with the ac system [20]. The main functions of DVR are:

(i) Reactive Power Compensation
(ii) Voltage Regulation
(iii) Compensation for Voltage sags and Swells

(iv) Unbalance Voltage Compensation (for 3-phase systems) The VSC generates a three phase ac output voltage which is controllable in phase and magnitude.

2.4.2 Capacitor banks

Nonlinear loads operating in electrical distribution systems generate harmonic currents that propagate throughout the network. As the harmonic order increases, the inductive reactance rises, while the capacitive reactance decreases. To achieve balance, capacitor banks must be installed in the system to equalize the inductive and capacitive reactance at a specific harmonic frequency. This balance occurs at a particular frequency known as the *resonant point*. Every system with a capacitor has both a parallel and a series resonant point. Harmonic frequencies that cause parallel resonance can amplify harmonic currents within the electric circuit, leading to significantly distorted voltages. Capacitor banks help to mitigate this by providing capacitive reactive power to balance out the inductive reactive power from inductive loads [15]. Depending on the system's needs, capacitor banks can either be fixed or switched to match the load's requirements [40].

2.4.3 Unified power flow controllers (UPFCs)

The shunt and series voltage-source converters are connected by a common DC link, which consists of a DC capacitor. This compensator hybrid combines shunt and series elements and eliminates the need for huge stored energy elements. Two voltage source inverters are part of UPFC. One injects a nearly sinusoidal voltage in series with the transmission line, while the other injects a nearly sinusoidal current at the connection's point of common coupling (PCC). Any angle between the injected voltage and the line current is acceptable. There are two components to the injected current. First, the injected voltage source plus losses in the UPFC negotiate the real component, which is in phase with the line voltage and provides or absorbs real power to the line. Second, the reactive component simulates an inductive or capacitive reactance at the connection site by being in quadrature with the line voltage. A voltage injection in series with the transmission line has been used to operate the SSSC model. Reactive current flow through the STATCOM model has been controlled, and switching between modes of operation occurs within a sub-cycle time. The model's functionality is confirmed by connecting it to a basic transmission line, which could be readily swapped out for the utility's current, more intricate power system network. In addition to compensating for reactive power, unified power quality conditioners (UPQC) provide the reduction of voltage and current disturbances that may impact delicate electrical loads. Combined series and shunt active power filters make up unified power quality conditioners (UPQC), which compensate for reactive power and voltage and current disturbances simultaneously. In transmission and distribution networks, UPFCs provide autonomous, adaptable control over the flow of both active and reactive electricity [7].

They are used to enhance voltage stability and manage the system's power flow. The function of UPQC includes

a) Reactive Power Compensation
b) Voltage Regulation
c) Compensation for Voltage sag and swell
d) Unbalance Compensation for current and voltage (for 3-phase systems)
e) Neutral Current Compensation (for 3-phase 4-wire systems)

The series converter performs the transmission line power flow with adjustable voltage magnitude and phase angle. Active power may flow in the series transformer and subsequently from or into the DC connection since there is no thermal constraint on the phase angle between the series voltage and the line current. The primary function of the shunt converter is to compensate for active power such that, in theory, the DC voltage remains constant by either withdrawing from or injecting into the AC side. Thus, the maximum active power flowing through the series transformer determines the shunt inverter's minimum rating. Theoretically, a rectifier could be used in place of the shunt converter if it were possible to ensure that the active power would always flow from the series converter to the line at any operational point of the series voltage and line current. But in this situation, the UPFC's operational range would be constrained. A common DC link capacitor connects the two solid-state voltage source inverters that make up the UPFC. Every inverter has a transformer connected to its output [7, 8].

2.4.4 Static Var compensators (SVCs)

A Static Var Compensator (SVC), as defined by IEEE, is an output-variable device that exchanges capacitive or inductive current to regulate or maintain specific characteristics of the electrical power system, especially bus voltages. SVCs are commonly employed to quickly stabilize voltage in areas of the network where it is weak. They are typically installed in load regions or along the middle of connecting transmission lines. The primary functions of Static Var Compensators are to improve power quality, regulate voltage within the distribution system, and enhance the transmission capacity of the power system. This is achieved by increasing stability margins and providing vital voltage support. The SVC operates as a voltage regulator, adjusting its Var output to rapidly reduce bus voltage fluctuations, particularly during and after significant power disturbances. This functionality improves transient stability and provides critical voltage support at the receiving end of the transmission line [28, 17].

2.4.5 D-STATCOM

A DSTATCOM is a controlled reactive source that can produce and/or absorb reactive power. It consists of a DC link capacitor and a voltage source converter (VSC) coupled in a shunt. The precise equivalent of the traditional rotating synchronous compensator serves as the foundation for the D_STATCOM's working principle. D-STATCOM is a power electronics-based, three-phase, shunt-connected device. It is connected to the distribution systems close to the load. A dc capacitor, a three-phase inverter (IGBT, thyristor) module, an ac filter, a coupling transformer, and a control scheme are the main parts of a D-STATCOM. The voltage-sourced inverter, which transforms an input DC voltage into a three-phase output voltage at fundamental frequency, is the primary electrical component of the D-STATCOM. To transform the DC link voltage Vdc on the capacitor into a voltage source with tunable magnitude and phase, D-STACOM uses an inverter. D_STATCOM can therefore be regarded as a voltage-controlled source. This shunt-controlled voltage source converter (VSC), which is based on a fast-response solid-state power electronic, injects current into the utility feeder or distribution system nodes for smooth reactive power compensation. This improves the power quality of the distribution system by, for example, improving the voltage profile and reducing power loss. A three-phase bus, shunt transformer, VSC, and DC capacitor make up D-STATCOM. Because the D-STATCOM is a voltage-sourced converter, its output voltage can be adjusted to meet reactive power requirements. Typically, a DC energy storage capacitor powers this gadget. In order to satisfy utility requirements, it produces both inductive and capacitive reactive power based on load demand [29, 18].

2.5 Electric system losses and voltage drop in transmission line

2.5.1 Electric system losses

Electric power must be transported via wires to the customers for consumption when it is produced at the generating location. For a variety of reasons, part of the power produced during this process is lost. The topic of contemporary energy efficiency concerns is whether or not this loss is at its lowest range. Technical and non-technical losses are two categories into which electric system losses can be separated to facilitate loss investigation [34].

2.5.1.1 Technical losses

A portion of the power is lost during the transition from the area of generation to the area of consumption due to the inherent characteristics of the equipment and conductors. On the one hand, technical losses over individual components reduce the elements' operational life; on the other hand, they require the power system to be more dimensioned. Technical losses can be categorized in a number of ways, including resistive, leakage, and corona losses, depending on where they originate. Leakage losses are losses brought on by the finite resistance of the insulating materials, whereas resistive losses, also known as copper losses, are I square R losses that are inherent in all conductors because of the conductors' finite resistance. Corona losses are caused by partial discharges in the air surrounding overhead lines [34].

2.5.1.2 Non- technical Losses

In actuality, these losses are not losses due to a decrease in consumption. The fact that the consumption is unpaid for is what qualifies them as losses. They can be assessed based on the computed technical losses on the one hand, and the difference between the energy generated and sold on the other. Non-technical losses are known to be caused by illegal energy use (theft), inaccurate meter readings, energy meter malfunctions, and billing errors [19, 34].

2.6 Factors influencing system losses

System losses are influenced by circulating current, phase balance, power factor, and voltage regulation. It is preferable to keep voltage restrictions for a transmission network within their rated values in order to reduce losses. Phase balancing systems can be used to balance heavily laden lines with other phases. There will be very little current flow at unity power factor, but any reactive component will raise the current, which will raise real power losses as well. When compared to unity power factor, the transmission network voltage decreases at the receiving end side and the voltage drop caused by line resistance is considerable as the transmission system's current increases. The system voltage profile must be maintained in order to minimize energy losses in transmission lines [19, 34].

2.7 Optimization Techniques

Since optimization's mathematical model is constrained, its primary goal is to maximize desired outcomes like profit, power quality, and efficiency or reduce unwanted outcomes like cost and energy loss. In literal terms, it refers to identifying the most optimal or preferred answer. From the perspective of optimization, a variety of approaches, including both conventional and contemporary optimization techniques, have been developed to address issues related to power system operation, control, and planning. The process of getting the optimal result under specific conditions is called optimization. There isn't a single, effective way to handle all optimization issues. As a result, several optimization techniques have been created to address various kinds of optimization issues. In every branch of engineering, optimization is a mathematical issue that is frequently faced. The application of scientific methods and procedures to decision-making problems and determining the best or optimal solutions is the focus of the mathematical field known as operations research [18, 21]. Moreover, there are three categories into which optimization techniques fall. Which include hybrid artificial intelligence tools, modernized optimization techniques, and classic methods [16].

Modernized optimization techniques include-

- Genetic algorithms
- Simulated annealing
- Particle swarm optimization,
- Ant colony optimization,
- Neural network-based optimization and
- Fuzzy optimization
- Grey wolf optimizer

CHAPTER THREE

MODELING AND METHODOLOGY

3.1 Research Methodology

The first step in this thesis project was to identify the core issue. A comprehensive review of existing literature followed, where relevant books, journals, essays, and theses on related topics were gathered. Data for the GERD to Holeta 500/400 kV Substation was collected and thoroughly analyzed. This data was then organized to facilitate its use in minimizing power loss and improving the voltage profile. A load flow study was conducted on the current transmission line network, GERD to Holeta 500/400 kV, under base-case operating conditions. The Newton – Raphson method algorithm was applied in the load flow analysis to determine the voltage profile at each bus and the power loss along the lines. After the installation of the Unified Power Flow Controller (UPFC) at the weak bus, another load flow analysis was performed using MATLAB 2016a software to assess bus voltage stability and power loss reduction. The Grey Wolf Optimization (GWO) algorithm was employed for this analysis to identify the optimal placement and size of the UPFC. The main goal of this study was to evaluate how effectively the UPFC reduces power loss, improves bus voltage profiles, and provides a cost-effective solution. Finally, the conclusions were drawn based on the results of the analysis.

.

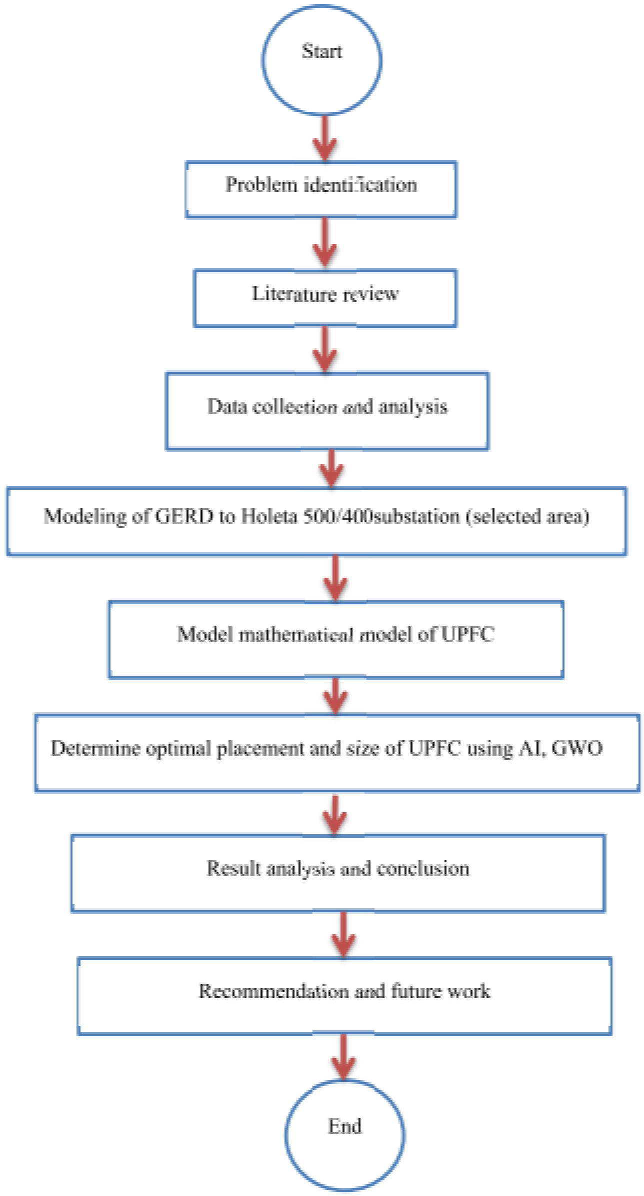

Figure3. 1 General methodology of thesis

Identification of the problem: state the problem that going to study and understand the problem**.**

Literature Review: referring different written things that deal with power system voltage profile index profile and voltage profile enhancement by using UPFC and how UPFC will work and its structure.

Collecting Data: collecting necessary data will related to the problem from the site in different ways these are through interviews, questionaries' and collecting measurement data.

Grey Wolf Optimization method algorithm implementation and simulation: this stage involves implementing GWO algorithm on MATLAB software to identify the optimal placement of UPFC. The simulation results will be evaluated and analyzed to measure the reduction in power loss and improvement in the voltage profile.

Sizing the UPFC: after the optimal placement of the UPFC the next stage is to rate it according to the feeder requirement.

Validation: this stage involves validating the results obtained from the simulation by comparing it with existing literature on this topic**.**

3.2 Data collected related to case area (GRED to Holeta 500/400 kv Power System Network)

The single-line diagram shown in Figure 3.2 represents the voltage levels of 500 kV and 400 kV. This system includes the GERD, DEDES

A, HOLETA, and HOLETA 400 kV buses. The transmission line from GERD to DEDESA spans 345 km and consists of four parallel lines. Similarly, the line from DEDESA to HOLETA is 275 km long, also with four parallel lines. The generators are modeled as synchronous machines with a salient pole rotor type. Key parameters for the generators include nominal power, line-to-line voltage, frequency, reactance, stator resistance (Rs), and time constants. Data for the HOLETA 500/400 kV substation, DEDESA 500/400 kV substation, GERD substation, and the power plant were collected. This data was gathered from the nameplates, drawings, and daily log sheets, in addition to communications with project offices and accessing various contractual agreements. Transmission line data, such as line length and impedance per kilometer, was also collected. Generator data for GERD was sourced from the contract documents and was used for simulation purposes.

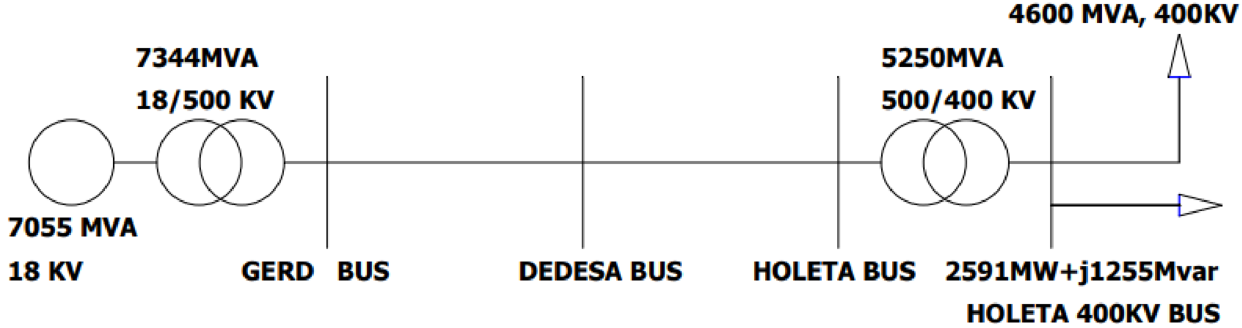

Figure3. 2 Single line diagrams of Holeta 500/400 kV substation

Table3. 1 Data of generators at GERD

Generator Type	Synchronous generator with salient poles	
Prime mover	Francis turbine	
Rated power output	444.4 MVA	
Rated stator voltage	18Kv	
Operating range of the stator voltage	± 5 %	
Rated frequency	50 Hz	
Rated power factor	0.9	
Number of phases	3	
Number of poles	48	
Rated speed	125 rpm	
Rated excitation current	2600 A	
Rated excitation voltage	353 V @ 130 °c	
Type of excitation	Static	
Continuous generator output charging a transmission line at a rated frequency	301.5 MVAr	
Reactance (in p.u. ref to 0.729 ohm)	Unsaturated	saturated
Xd	1.208	0.986
x’d	0.314	0.820
x’’d	0.265	0.194
Xq	0.820	
x’q	0.820	
x’’q	0.3350.307	
x2	0.296	
x0	0.092	
Time constants		
T’d0	10.30 s	
T’d	2.675 s	
T’’d	0.054 s	
T’’d0	0.064 s	
T’’q	0.001 s	

T''q0	0.003 s
Ta	0.362 s
Stator winding resistance(3 phase in series)	4.67 mΩ
Rotor winding resistance	94.91 mΩ
Stator winding capacitance	2.20 µF per phase

3.2.1 Existing voltage profile of HOLETA 500/400 kV KV Holeta bus bar

The recorded data from the Holeta 500/400 kV substation spans a duration of one year, but the data presented here covers the first six months (September 2023 to March 2024). The data indicates that the voltage profile fluctuated between maximum and minimum values. This resulted in both overvoltage and under voltage (sag) issues. The problem of overvoltage and under voltage will be addressed by the smooth operation of the UPFC at the Holeta 500/400 kV substation. The primary objective of this study is to evaluate the capability of the UPFC in enhancing power evacuation and improving voltage stability within the network. The recorded data is presented graphically below.

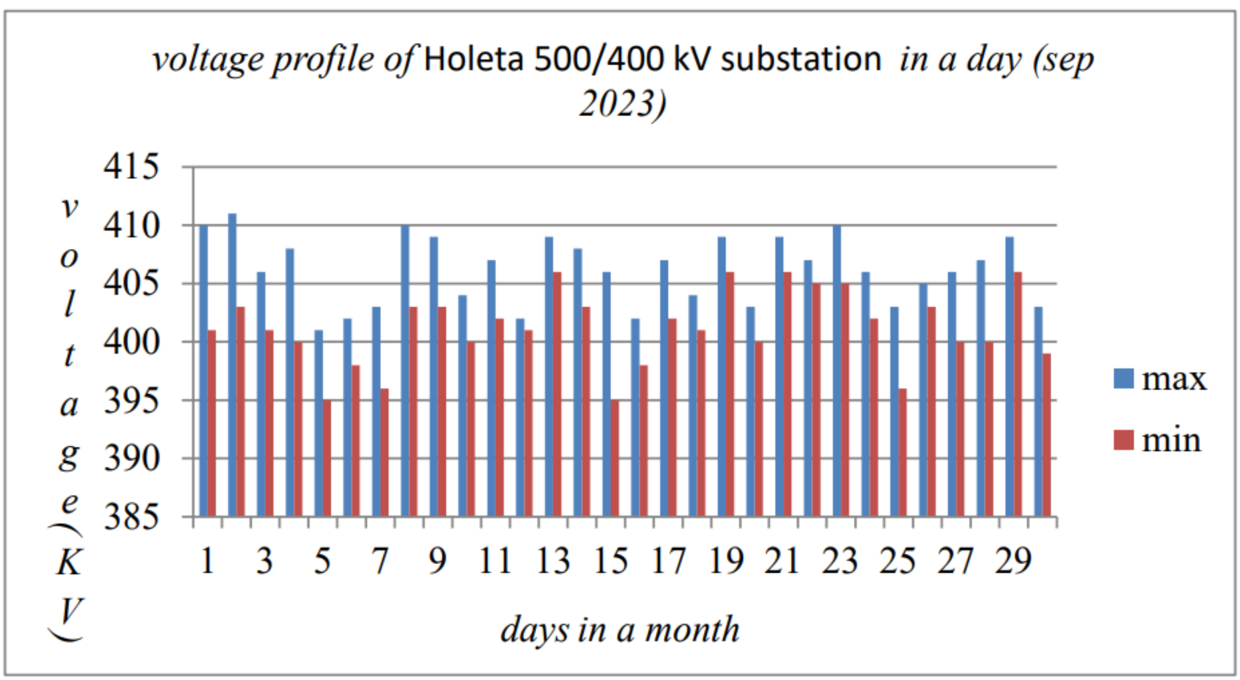

Figure3. 3 voltage profile of holeta 500/400 KV substation (Sep 2023)

From the data taken on the actual reading of the 24 hour working SCADA system of the substation in Sep 2023 the voltage profile was oscillating between 412 kv and394 kv.

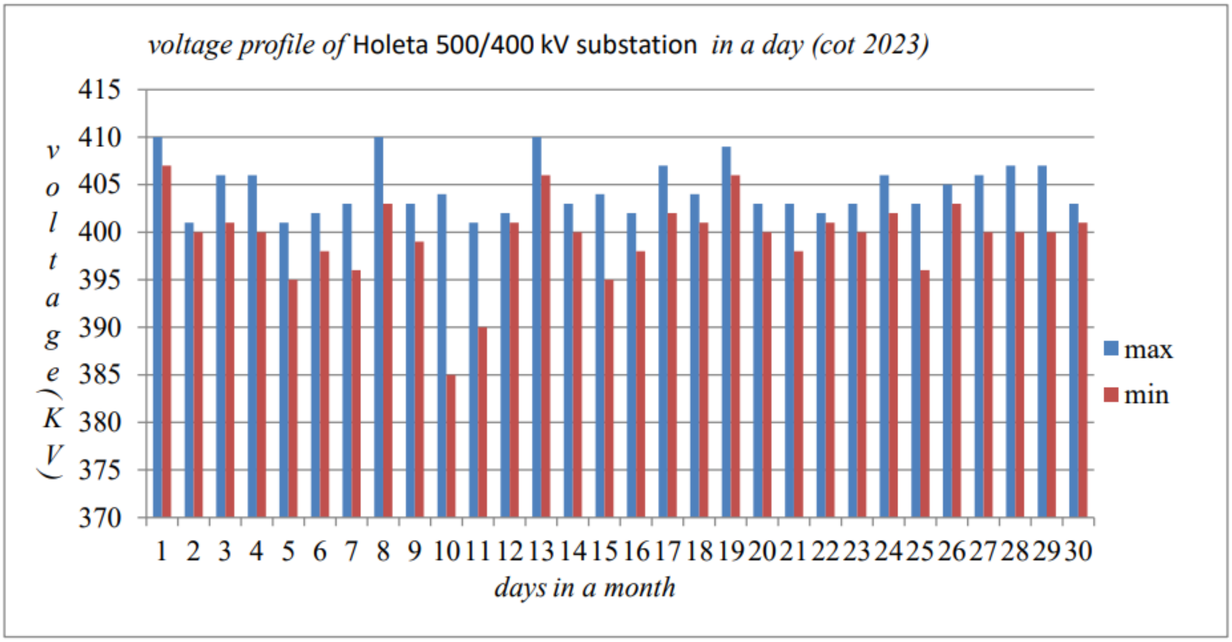

Figure3. 4 voltage profile of holeta 500/400 KV substation (Oct 2023)

From the data taken on the actual reading of the 24 hour working SCADA system of the substation in October 2023 the voltage profile was oscillating between 410 kv and385 kv.

From the data taken on the actual reading of the 24 hour working SCADA system of the substation in November 2023 the voltage profile was oscillating between 413 kv and 386 kv.

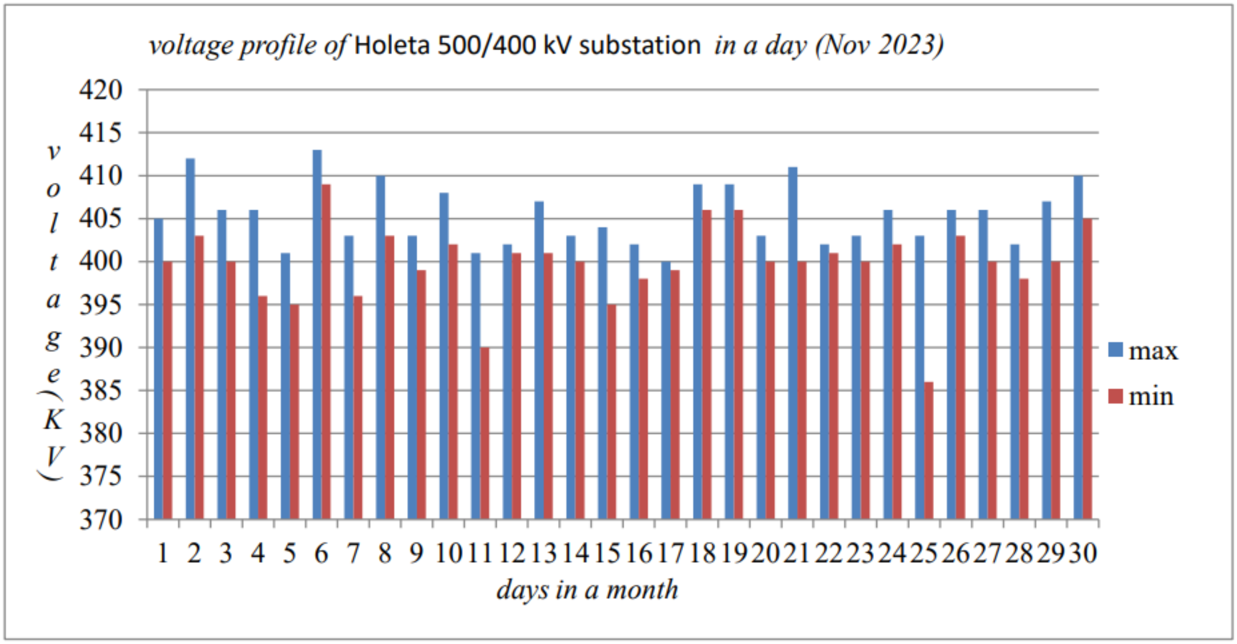

Figure3. 5 voltage profile of holeta 500/400 KV substation (Nov 2023)

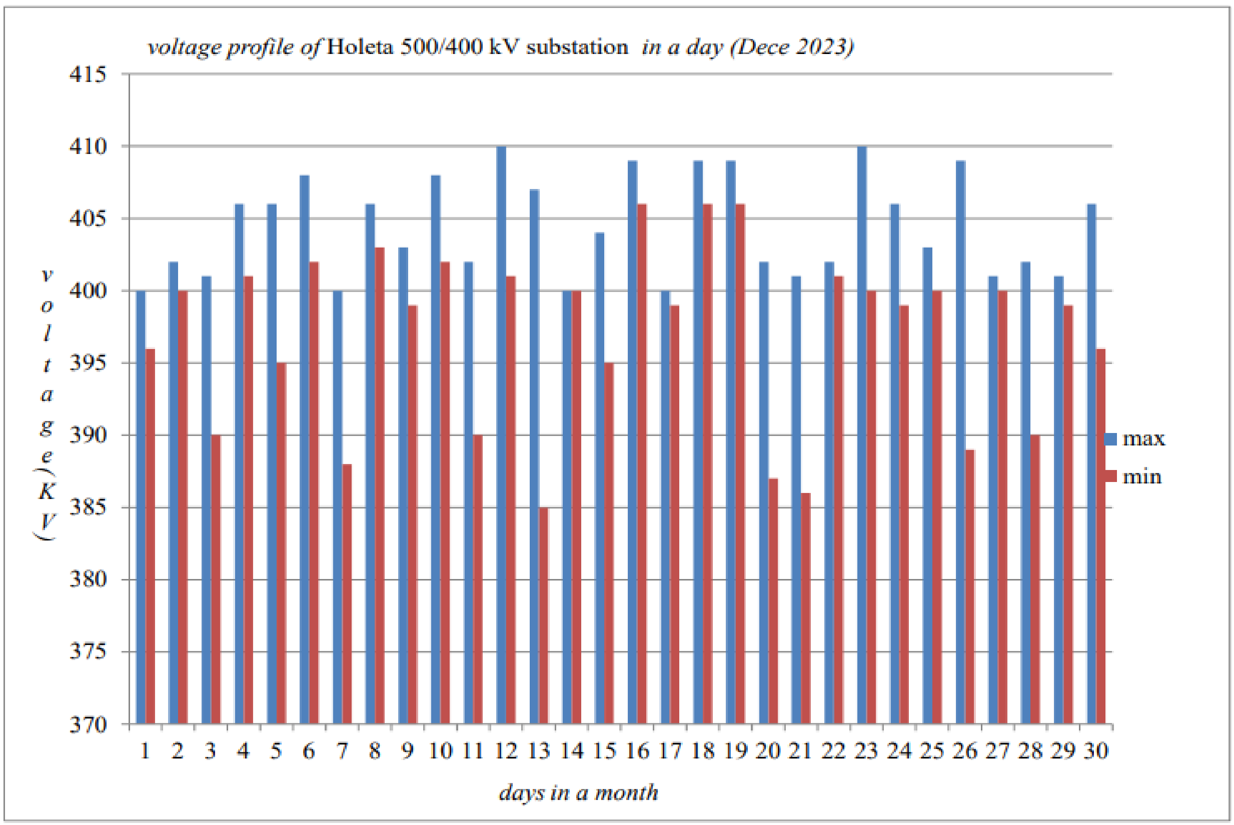

Figure3. 6 voltage profile of holeta 500/400 KV substation (Dece 2023)

From the data taken on the actual reading of the 24 hour working SCADA system of the substation in December 2023 the voltage profile was oscillating between 413 kv and 386 kv.

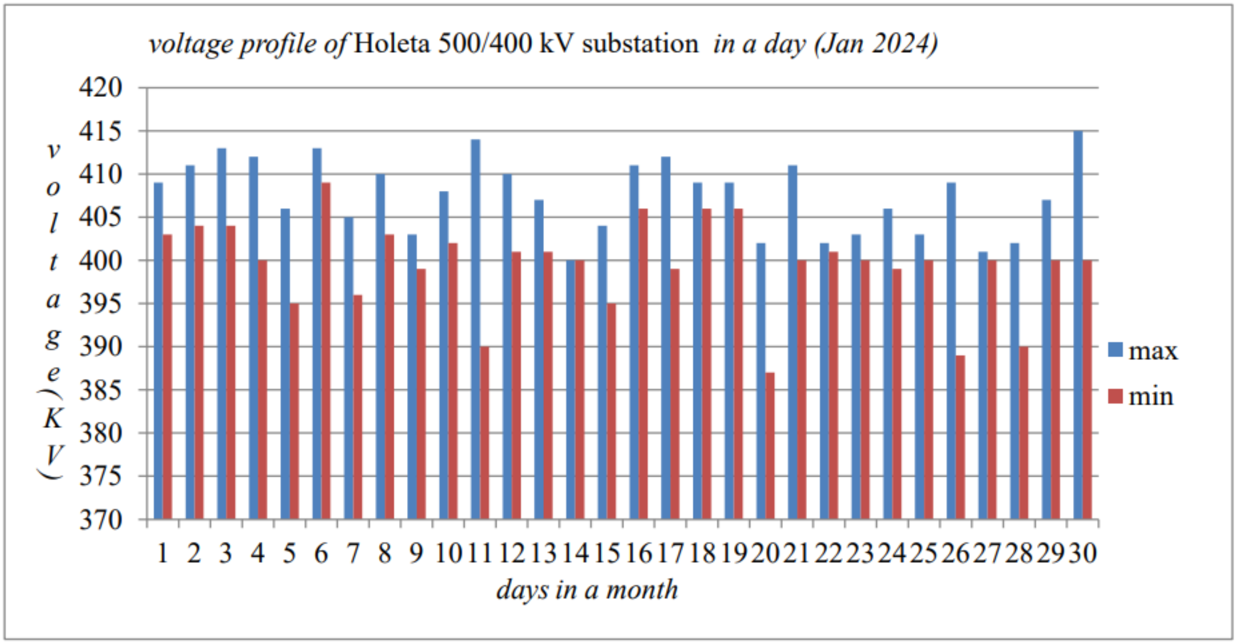

Figure3. 7 voltage profile of holeta 500/400 KV substation (Jan 2023)

From the data taken on the actual reading of the 24 hour working SCADA system of the substation in January 2024 the voltage profile was oscillating between 415 kv and 386 kv.

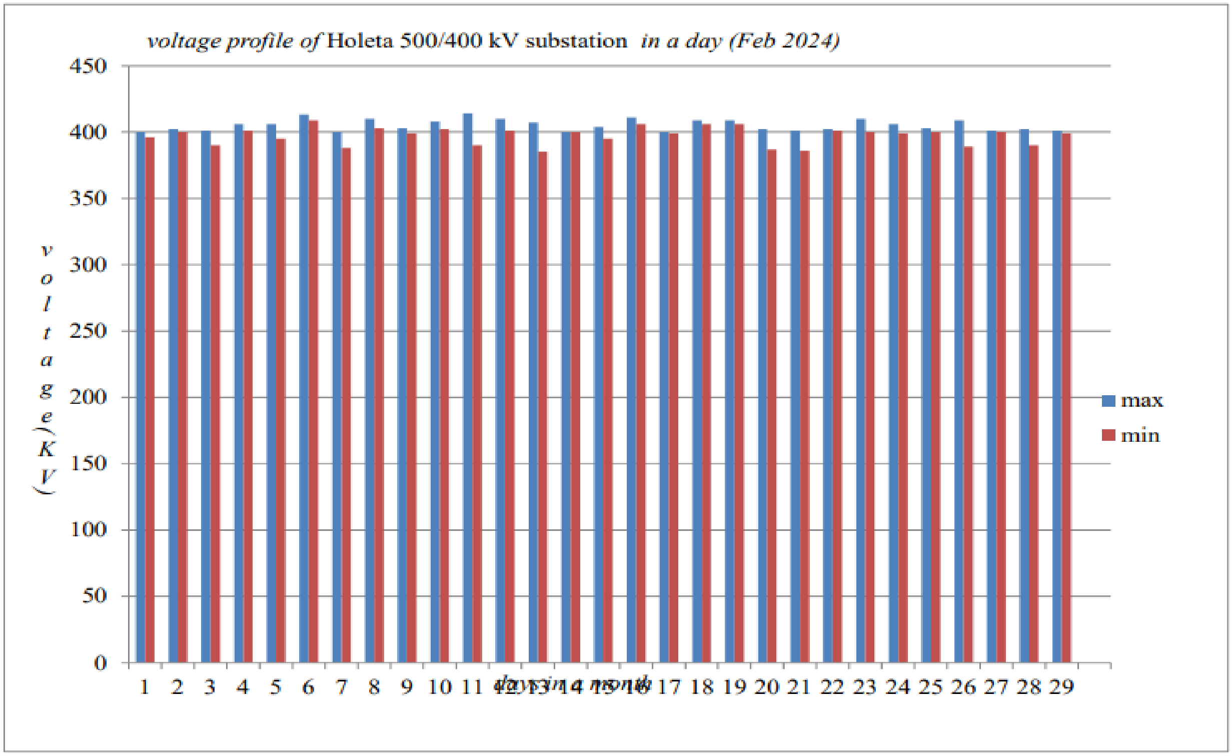

Figure3. 8 voltage profile of holeta 500/400 KV substation (Feb 2023)

From the data taken on the actual reading of the 24 hour working SCADA system of the substation in February 2024 the voltage profile was oscillating between 415 kv and 386 kv.

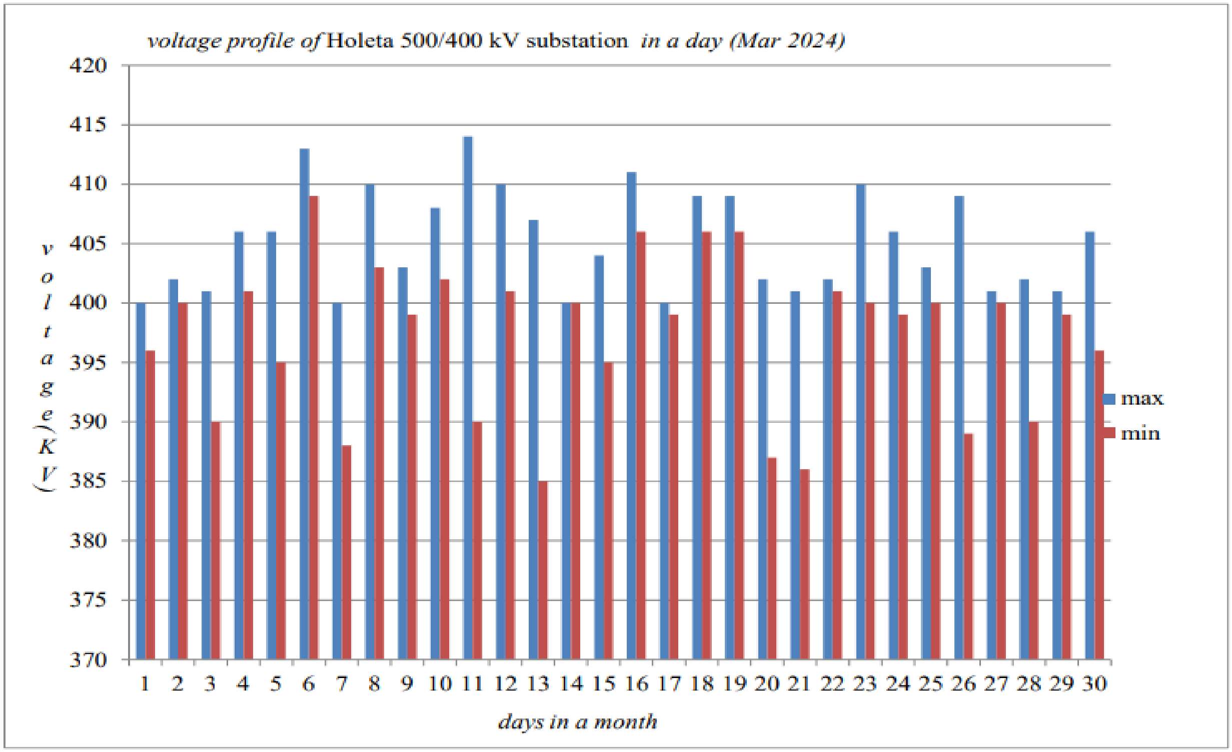

Figure3. 9 voltage profile of holeta 500/400 KV substation (Mar 2023)

From the data taken on the actual reading of the 24 hour working SCADA system of the substation in March 2024 the voltage profile was oscillating between 414 kv and 385 kv.

3.3 Unified Power Flow Controller (UPFC) and Topology

Hybrid compensators, known as Unified Power Flow Controllers (UPFC), are based on voltage-source converters. With the deregulation of transmission services, the UPFC's ability to independently and simultaneously control both active and reactive power in a transmission line, without requiring large energy storage components, has become a notable advantage. The primary function of the UPFC is to independently adjust both active and reactive power at a specific transmission line node. It consists of shunt and series forced commutated voltage-source converters coupled to a common DC link [22]. The series converter controls the flow of electricity by providing a three-phase series voltage with variable magnitude and phase along the transmission line. Active power can flow through the series transformer and into or out of the DC link, as there are no phase angle restrictions between the series voltage and the line current. The main role of the shunt converter is to compensate for this active power by either injecting into or withdrawing from the AC side, thereby maintaining a constant DC voltage. The shunt converter's minimum rating is determined by the maximum active power flowing through the series transformer. In theory, the shunt converter could be replaced by a series converter if it were ensured that active power would always flow from the converter to the line at all operational points of the series voltage and line current. However, this would limit the operational range of the UPFC [7, 24]. The UPFC is capable of simultaneously controlling the transmission line's phase angle, impedance, and voltage. It contains two switching converters, powered by a common DC link provided by a DC storage capacitor. One converter manages the power flow of the UPFC by injecting an AC voltage (Vpq) with a programmable magnitude and phase angle in series with the transmission line through a series transformer. The other converter handles shunt reactive power adjustments and absorbs or produces controlled reactive power [3, 23]. In the power system industry, the UPFC, which integrates the functions of the SSSC and STATCOM, is used to enhance stability. It regulates various parameters such as the transmission line’s voltage, magnitude, active power, and reactive power. Consequently, FACTS devices like the UPFC play a crucial role in improving voltage stability and overall transmission line performance [17].

The main challenges where the capabilities and use of FACTS (Flexible AC Transmission Systems) devices are observed include line outages, congestion, cascade line tripping, and the loss of power system stability. The Unified Power Flow Controller (UPFC) is a notable example of a FACTS device from the previous generation. UPFC can simultaneously control all three key line power flow parameters—line impedance, voltage, and phase angle. It combines the functionalities of two older FACTS devices: the Static Synchronous Compensator (STATCOM) and the Static Synchronous Series Compensator (SSSC). These two devices are essentially Voltage Source Inverters (VSIs) connected via a common DC link that includes a storage capacitor. The STATCOM is connected in shunt with the transmission line, while the SSSC is c0onnected in series with the line via a series transformer. The shunt inverter helps balance the real power exchanged between the transmission line and the series inverter, and it regulates the voltage at the point of connection by injecting reactive power into the line. On the other hand, the series inverter regulates the active and reactive power flow in the line by injecting a voltage with a regulated magnitude and phase. By using both shunt and series components, the UPFC can effectively manage both current and voltage in the system.

The UPFC is a powerful and adaptable FACTS device, often referred to as the most complete multivariable FACTS controller. It can control both real and reactive power flow, as well as voltage amplitude, at the point of common coupling, either selectively or simultaneously. The challenge of using UPFC to simultaneously manage multiple power system variables arises from the interactions between these variables, making UPFC control complex. The combination of STATCOM and SSSC through a common DC link enables bidirectional real power flow between the series output terminals of the SSSC and the shunt output terminals of the STATCOM. This configuration provides real and reactive series line compensation without the need for an external electric energy source, which further enhances the device's efficiency and flexibility in power system operation [4].

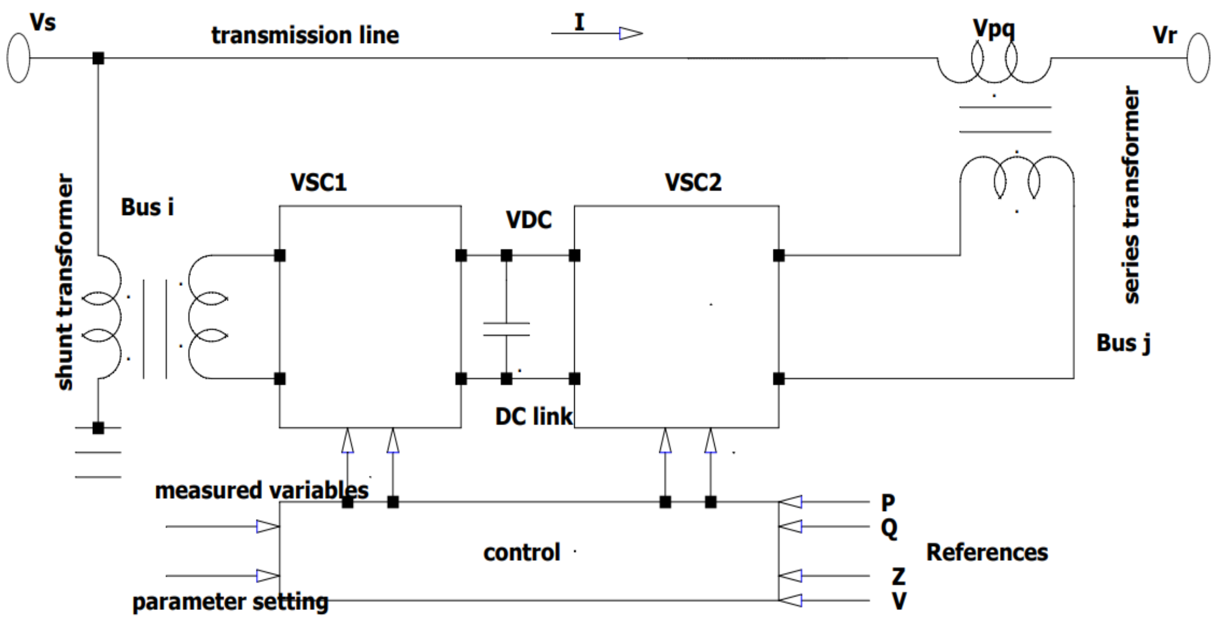

Figure3. 10 Basic Circuit arrangement of UPFC

3.4 Mathematical Modeling and Injection Model of Unified Power Flow Controller (UPFC)

In the steady-state operation of the power system with the Unified Power Flow Controller (UPFC), an injection model is derived for this thesis. Under steady-state conditions, the UPFC can be represented by two voltage source converters, which capture the fundamental components of the output voltage waveforms of both converters, with the impedance modeled as the leakage reactance of the two coupling transformers. This representation helps in understanding the impact of UPFC on the transmission network during steady-state operation. Additionally, the UPFC injection model can be seamlessly integrated into the steady-state power flow model [13].

The UPFC, which consists of two switching converters operating from a common DC link, is modeled using a steady-state injection approach. The series converter of the UPFC is assumed to be connected between buses i and j, with sending voltage vsv_svs and receiving voltage vrv_rvr, respectively. The series converter injects an AC voltage VVV with a controllable magnitude and phase angle in series with the transmission line. The shunt converter, on the other hand, injects or absorbs reactive power independently at bus-i, and it also supplies or absorbs the active power demanded by the series converter through the common DC link [30].

The UPFC controller consists of two components: the series and shunt controllers. The series component injects a series voltage into the system, while the shunt component injects a current into the system [31].

3.4.1 Injection Model of Unified Power Flow Controller

For this thesis, at steady state power system operation the UPFC injection model is derived. And also in steady state condition UPFC can be represent by two voltage sources converters which is representing fundamental components of output voltage waveforms of the two converters and impedances being leakage reactance of the two coupling transformers. The impact of UPFC on transmission network at steady state condition is understandable by using this model. Furthermore, the UPFC injection model can be easily integrated in the steady state power flow model [13]. Figure bellow shows that the two voltage –source model of UPFC.

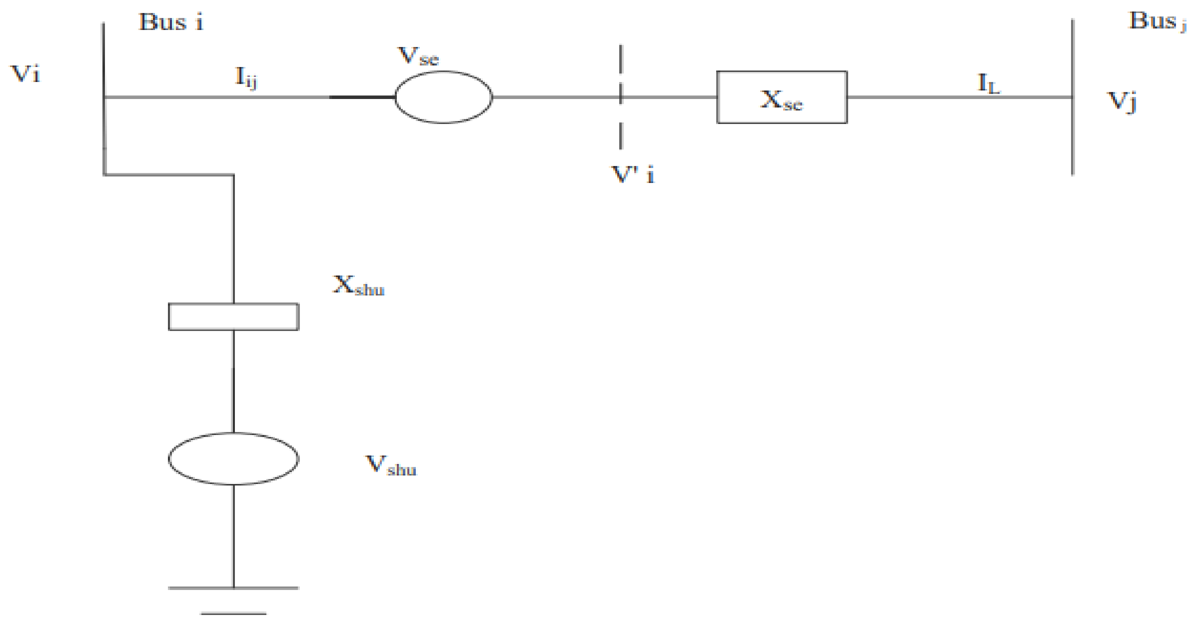

Figure3. 11Voltage source model of UPFC [13]

Considering Bus-i voltage as reference V_i= │V│$\angle 0^0$. All other remaining bus voltage angles are taken with respect to this bus angle. The voltage source, V_{se} and $V_{shu}$are controllable in both magnitude as well as phase angle. Then, the voltage up to UPFC is given by,

$$V_i + V_{se} = V' \qquad (3.1)$$

Therefore, the series voltage source V_{se} is controllable in magnitude and phase and can be given by:

$$V_{se} = r\, V_i e^{i\gamma} \qquad (3.2)$$

Where, $0 < r < r_{max}$ and $0 < \gamma < 2\pi$

r and γ are the values of Series voltage Source coefficient and Series Voltage Source angle respectively.

Basically UPFC injection model consist two voltage source converter models; series connected voltage source converter model as well as shunt connected voltage source converter model. The power fed by the UPFC can be determined by using superposition theorem. Modeling of both converter models (series and shunt) converter modes are discussed here briefly [13].

3.4.1.1 Series Connected Voltage Source Converter Model

On the basis of a vectorial representation, a mathematical model for the series VSC is created. The d-q components of the inserted series voltage are the control output variables, and the d-q components of the line current are the variables to be controlled. It is believed that the PWM switching strategy corrects changes in the DC link voltage, therefore it has no effect on the control system's calculation of the series voltage reference. Finding an appropriate and straightforward controller for the series converter is the goal of the mathematical model's derivation [7]. The figure below (fig 3.3) shows series connected voltage source converter. By considering this series connected voltage source which is located between bus-i and bus-j in a power system, series voltage source converter can be modeled with an ideal series voltage V_{se} in series with a reactance X_{se} [13].

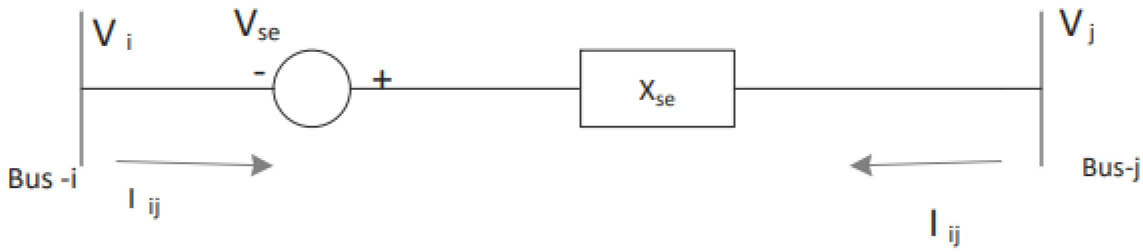

Figure3. 12 Series connected Voltage source converter (VSC)

Replacement of Series Voltage Source by Current Source is shown in figure below (figure 3.4) in this replacement current source is connected in parallel with the transmission line.

$I_{se} = -jb_{se}V_{se}$ (3.3)

Where, b_{se}= 1/ X_{se} (3.4)

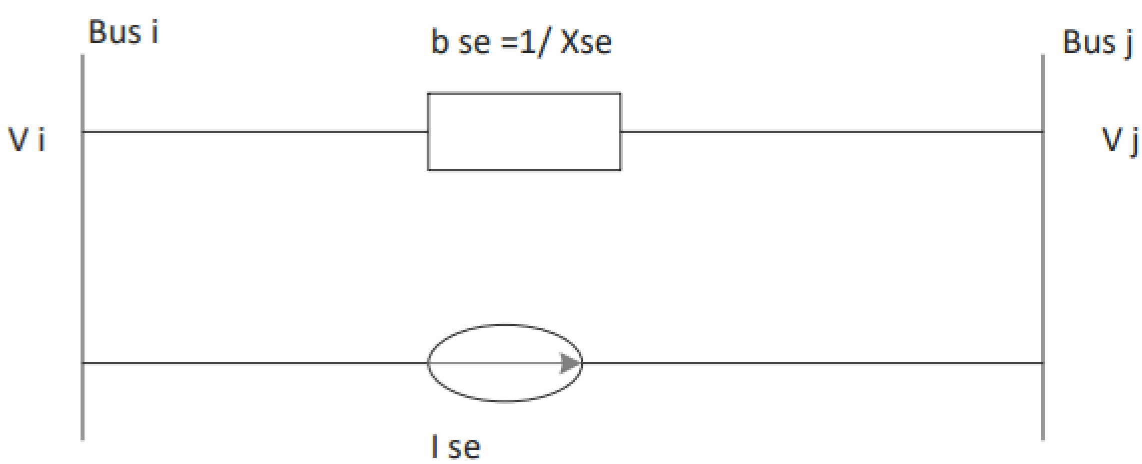

Figure3. 13 Replacement of Series Voltage Source by Current Source [13]

From above figure 3.4, the current source I_{se} can be modeled by injection powers S_{ise} and S_{jse} at the two buses which are expressed by

$S_{ise} = V_i(-I_{se})^*$ (3.5)

$S_{jse} = V_j(I_{se})^*$ (3.6)

By substituting equations 3.3 and 3.4 into equation 3.5 injected powers S_{jse} can be simplified as,

$S_{ise} = V_i(b_{se}\mathrm{r}V_i je^{i\gamma})*$ (3.7)

$S_{ise} = V_i(-b_{se}\mathrm{r}V_i je^{i\gamma})*$ (3.8)

Where −j = e −j90 (3.9)

Substituting equation 3.9 in to 3.8,

$S_{ise} = V_i\ (b_{se}\mathrm{r}V_i * e - (\gamma+90)\ )$ (3.10)

By using Euler Identity, i.e. $je^{i\gamma}$ = cos γ + j sin γ, equation 3.10 cab simplified as,

$S_{ise} = V_i^2 b_{se}$ r (cos (−γ − 90) + j sin (−γ − 90)) (3.11)

As cos (−γ − 90) = − sin γ and sin (−γ − 90) = − cos γ

By using trigonometric identities equation 3.11 can be simplified as,

$S_{ise} = -\mathrm{r}b_{se}\ V_i^2 \sin\gamma - \mathrm{j}\mathrm{r}b_{se}V_i^2 \cos\gamma$ (3.12)

Since $S_{ise} = P_{ise} + \mathrm{j}Q_{ise}$, then separating the real and imaginary part,

$P_{ise} = -\mathrm{r}b_{se}\ V_i^2 \sin\gamma)$ (3.13)

$Q_{ise} = -\mathrm{r}b_{se}\ V_i^2 \cos\gamma$ (3.14)

Similarly, substituting equation 3.2 and 3.3 into equation 3.6the injected power S_{ise}can be modified as,

$S_{jse} = V_i(-b_{se}\mathrm{r}V_i je^{i\gamma})*$ (3.15)

But the voltage at each bus is given by $V_j = V_j\angle\theta\mathrm{j}$ and $V_i = V_i\angle\theta\mathrm{i}$

$S_{jse} = V_i\angle\theta\mathrm{i}\ (-b_{se}\mathrm{r}V_i je^{i\gamma})*$ (3.16)

$S_{jse} = V_j e^{j\theta\mathrm{j}}\ (-jb_{se}\mathrm{r}V_i e^{j\theta\mathrm{i}}e^{i\gamma})\ *$ (3.17)

$S_{jse} = V_j e^{j\theta\mathrm{j}}\ b_{se}\mathrm{jr}V_i^* e^{-j\theta\mathrm{i}}e^{-i\gamma}$ (3.18)

$S_{jse} = e^{j90}V_j e^{j\theta\mathrm{j}}\ b_{se}\mathrm{r}V_i^* e^{-j\theta\mathrm{i}}e^{-i\gamma}$ (3.19)

Where, j = e^{j90}

$S_{jse} = rV_jV_ib_{se}e(^{j(90+\theta j-\theta i-\gamma)})$ (3.20)

$S_{jse} = rV_jV_ib_{se}$ (cos (90 + θ_j − θ_i − γ) + j sin (90 + θ_j − θ_i − γ)) (3.21)

$S_{jse} = rV_jV_ib_{se}$ (cos (90 − (−θ_j + θ_i + γ)) + j sin (90 − (−θ_j + θ_i + γ))) (3.22)

Cos (90 − (−θ_j + θ_i + γ)) = cos 90 cos (−θ_j + θ_i + γ) + sin 90 sin (−θ_j + θ_i + γ) (3.23)

= Sin (−θ_j + θ_i + γ) (3.24)

And

$$\text{Sin}\,(90 - (-\theta_j + \theta_i + \gamma)) = \sin 90 \cos(-\theta_j + \theta_i + \gamma) + \sin(-\theta_j + \theta_i + \gamma) \cos 90 \quad (3.25)$$

$$= \text{Cos}\,(-\theta_j + \theta_i + \gamma) \quad (3.26)$$

Then by substituting equation 3.24 and 3.25 into equation 3.22 and equation 3.22 is simplified as,

$$S_{jse} = rV_jV_ib_{se}\sin(\theta_i - \theta_j + \gamma) + jrV_jV_ib_{se}\cos(\theta_i - \theta_j + \gamma) \quad (3.27)$$

But $\theta_{ij} = \theta_i - \theta_j$ substituting this values into equation 3.27 then the final equation can be written as,

$$S_{jse} = rV_jV_ib_{se}\sin(\theta_{ij} + \gamma) + jrV_jV_ib_{se}\sin\cos(\theta_{ij} + \gamma) \quad (3.28)$$

Since

$$S_{jse} = P_{jse} + jQ_{jse}, \quad (3.29)$$

Then separating the real and imaginary part,

$$P_{jse} = rV_jV_ib_{se}\sin(\theta_{ij} + \gamma) \quad (3.29)$$

$$Q_{jse} = rV_jV_ib_{se}\cos(\theta_{ij} + \gamma) \quad (3.30)$$

The power injection model of the series connected voltage source can be seen as two independent loads at the buses i and j as shown in figure below.

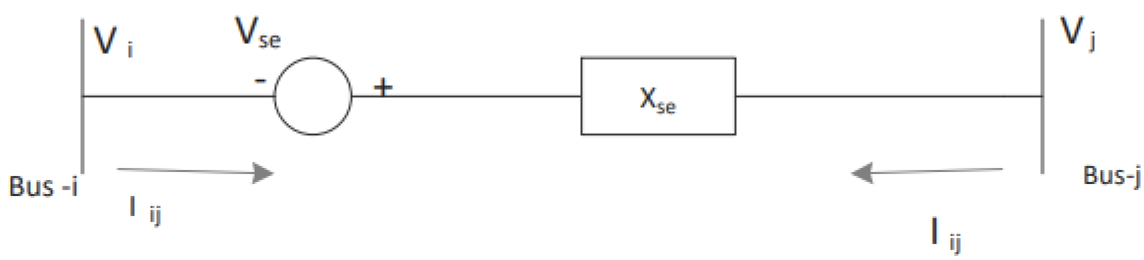

Figure3. 14 Power injection model for a series connected VSC [13]

$$P_{ise} = -rb_{se}V_i^2 \sin\gamma \quad (3.31)$$

$$P_{jse} = rV_jV_ib_{se}\sin(\theta_{ij} + \gamma) \quad (3.32)$$

$$Q_{ise} = -rb_{se}V_i^2 \cos\gamma \quad (3.33)$$

$$Q_{jse} = rV_jV_ib_{se}\cos(\theta_{ij} + \gamma) \quad (3.34)$$

3.4.1.2 Shunt Connected Voltage Source Converter Model

The shunt-connected converter of UPFC is used mainly in order to provide both the active power demand of the series connected voltage source converter, which is injected to the system, and the losses within the UPFC. The total switching of the two converters is estimated to be about 2% of the power transfer for the converters. If the losses in the active power injection of the shunt connected voltage source converter at bus-i, $P_{conv\ 1}$ is equal to 1.02 times the injected series active power $P_{conv\ 2}$ through the series connected voltage source converter to the system [13].

$$P_{conv\ 1} = -1.02\ P_{conv\ 2} \quad (3.35)$$

The apparent power supplied by the series converter is given by,

$$S_{conv\ 2} = V_{se} I_{ij}\ * \quad (3.36)$$

$$I_{ij} = \frac{V_i' - V_j}{jX_{se}} \quad (3.37)$$

Substituting equation 3.2 and 3.37 into equation 3.36 it is modified as,

$$S_{conv\ 2} = rV_i e^{i\gamma}\ (\frac{V_i' - V_j}{jX_{se}})* \quad (3.38)$$

Substituting equation 3.1 into equation 3.38 it is simplified as,

$$S_{conv\ 2} = rV_i e^{i\gamma}\ (\frac{V_i + V_{se} - V_j}{jX_{se}})* \quad (3.39)$$

Again substituting equation 3.2 into equation 3.39 it is simplified as,

$$S_{conv\ 2} = rV_i e^{i\gamma}\ (\frac{V_i + rV_i e^{i\gamma} - V_j}{jX_{se}})* \quad (3.40)$$

But the voltage at each bus is given by V_j = $V_j \angle \theta j$ and V_i = $V_i \angle \theta i$

$$S_{conv\ 2} = r\ V_i \angle \theta \mathrm{i} e^{i\gamma}\ (\frac{V_i \angle \theta + rV_i \angle \theta e^{i\gamma} - V_j \angle \theta \mathrm{j}}{jX_{se}})* \quad (3.41)$$

$$S_{conv\ 2} = \ r\ V_i e^{i\gamma} e^{j\theta \mathrm{i}} (\frac{V_i e^{j\theta \mathrm{i}} + rV_i e^{j\theta \mathrm{i}} e^{i\gamma} - V_j e^{j\theta \mathrm{j}}}{jX_{se}}) \quad (3.42)$$

$$S_{conv\ 2} = \ r\ V_i e^{i\gamma} e^{j\theta \mathrm{i}} (\frac{V_i e^{-j\theta \mathrm{i}} + rV_i e^{-j\theta \mathrm{i}} e^{i\gamma} - V_j e^{-j\theta \mathrm{j}}}{-jX_{se}}) \quad (3.43)$$

Substituting bse = 1/ X_{se} in to the above equation 3.43 it gives,

$$S_{conv\ 2} = \ r\ b_{se} V_i e^{j(\theta \mathrm{i} + \gamma)}\ (\frac{V_i e^{-j\theta \mathrm{i}} + rV_i e^{-j(\theta \mathrm{i} + \gamma)} - V_j e^{-j\theta \mathrm{j}}}{-j}) \quad (3.44)$$

Multiplying the numerator and denominator of equation 3.44 by conjugate of $-j$ and it can be simplified as,

$$S_{conv\ 2} = r\ b_{se} V_i e^{j(\theta \mathrm{i} + \gamma)} (V_i e^{-j\theta \mathrm{i}} + rV_i e^{-j(\theta \mathrm{i} + \gamma)} - V_j e^{-j\theta \mathrm{j}}) \quad (3.45)$$

Then the above equation can be simplified as,

$$S_{conv\ 2} = \ \mathrm{j} r b_{se} V_i^2 e^{\mathrm{j}\gamma} + \ jr^2\ b_{se} V_i^2 - rjb_{se} V_i V_j e^{j(\theta_i - \theta_j + \gamma)} \quad (3.46)$$

By using Euler identity, i.e. $e^{i\gamma}$= cos γ + j sin γ

And

$e^{j(\theta_i-\theta_j+\gamma)}$ = cos $(\theta_i - \theta_j + \gamma)$ +j sin $(\theta_i - \theta_j + \gamma)$ then equation (3.46) is simplified as,

$$S_{conv\,2} = \text{j}rb_{se}V_i^2(\cos\gamma + \text{j}\sin\gamma) + jr^2 b_{se}V_i^2 - rjb_{se}V_iV_j(\cos(\theta_i - \theta_j + \gamma) + \text{j}\sin(\theta_i - \theta_j + \gamma)) \quad (3.47)$$

Therefore, separating the real and imaginary part the active power and reactive power at converter-2 as follows,

$$P_{conv\,2} = r\, b_{se}V_iV_j\sin(\theta_i - \theta_j + \gamma) - \text{r}b_{se}V_i^2\sin\gamma \quad (3.48)$$

$$Q_{conv\,2} = r\, b_{se}V_iV_j\cos(\theta_i - \theta_j + \gamma) - \text{r}b_{se}V_i^2\cos\gamma + r^2b_{se}V_i^2 \quad (3.49)$$

Then the active power injected at converter-1 is determine by substituting equation 3.48 into equation 3.31 as,

$$P_{conv\,1} = -1.02\, r\, b_{se}V_iV_j\sin(\theta_i - \theta_j + \gamma) + 1.02\,\text{r}b_{se}V_i^2\sin\gamma \quad (3.50)$$

The reactive power delivered or absorbed by voltage source converter 1 is independently controllable by UPFC and can be modeled as a separate controllable shunt reactive source. In the view of above, it is assumed that the reactive power of converter-1 is equal to zero. The UPFC injection model is constructed from the series connected voltage source converter model with the addition of a power equivalent to Pconv1 + j0 to bus-i [13].

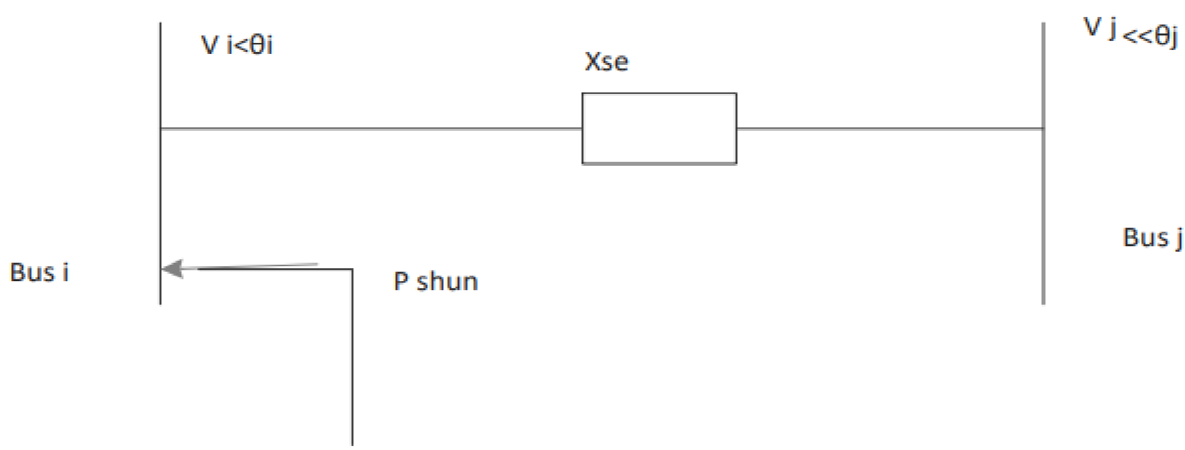

Figure3. 15 shunt connected voltage source converter of Power injection model

Finally, the steady-state UPFC mathematical modeling can be constructed by combining the series power injection and shunt power injection at bus-i and bus-j. The element of power injection model of UPFC can be expressed as follows,

$$P_{i\,UPFC} = -r\, b_{se}V_i^2\sin\gamma - 1.02\text{r}b_{se}V_iV_j\sin(\theta_i - \theta_j + \gamma) + 1.02\text{r}b_{se}V_i^2\sin\gamma$$

$$= 0.02\text{r}b_{se}V_i^2\sin\gamma - 1.02\text{r}b_{se}V_iV_j\sin(\theta_i - \theta_j + \gamma) \quad (3.51)$$

$$Q_{i\,UPFC} = -\mathrm{r}b_{se}V_i^2 cos\,\gamma \quad (3.52)$$

$$P_{jUPFC} = rb_{se}\, V_iV_j \sin(\theta_i - \theta_j + \gamma) \quad (3.53)$$

$$Q_{jUPFC} = rb_{se}\, V_iV_j \sin(\theta_i - \theta_j + \gamma) \quad (3.54)$$

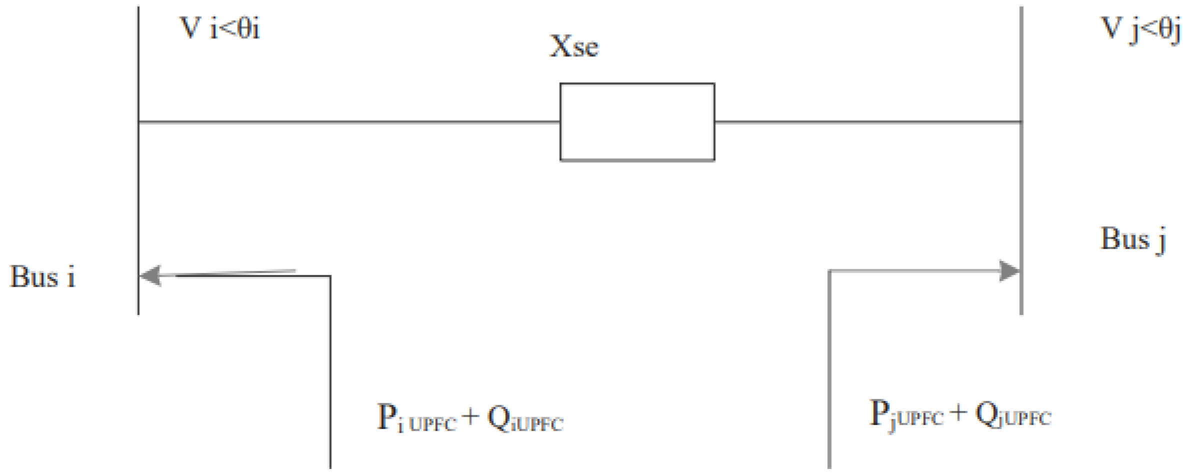

Figure3. 16 the overall System steady state UPFC mathematical model [13]

3.5 Power Flow Analysis of GERD to HOLETA Transmission line network without UPFC.

Load flow studies, also known as power flow studies, are an important component of power system analysis. They are required for existing system planning, economic scheduling, and control, as well as future growth planning. The task entails calculating the magnitudes and phase angles of voltages at each bus, as well as the active and reactive power flow in each line [35].

When the injecting complex power is defined, power system load flow calculations can be thought of as the problem of calculating the node voltage phasor for each node. If the complex power can be represented by equations of complex voltages, the node voltage phasors can be solved using a nonlinear equation solving approach like the Newton Raphson method. The foundation for solving performance equations in computer aided electrical power system analyses, such as load flow analysis, is a mathematical analysis relating the solution of arithmetic simultaneous equations.

Forming the Y-bus admittance with the transmission line and transformer input data is the first step in performing load flow analysis. The following is the nodal equation for a power system grid using Y bus:

I=Y bus *V (3.55)

The nodal equation can be inscribed in a comprehensive form for an n bus system

$I_i = \sum_{j=1}^{n} Y_{ij} V_j$ For i=1,2…n (3.56)

The complex power delivered to bus i is

$P_i + jQ_i = V_i I_i$ (3.57)

$$Ii = \frac{Pi\text{-}jQi}{*Vi} \quad (3.58)$$

Substituting for Ii in terms of $Pi and\ Qi$, the equation gives

$$\frac{Pi\text{-}jQi}{*Vi} = Vi \sum_{j=1}^{n} yij - \sum_{j=1}^{n} yijVj \quad j \neq i \quad (3.59)$$

This is equation (3.5) uses iterative techniques to solve load flow problems.

3.5.1 Newton-Raphson Method

The technique was termed after Isaac Newton and Joseph Raphson. It is an iterative technique that uses Taylor's series expansion to convert a collection of non-linear simultaneous equations to a set of linear simultaneous equations, with the terms constrained to the initial approximation. The Newton-Raphson approach is the most iterative technique used for load flow because its convergence features are comparatively more powerful than other alternate methods, and the consistency of the Newton-Raphson approach is relatively good because it can solve cases that cause divergence with other common methods.

If the assumed value is close to the solution, the result is achieved quickly; but, if the supposed value is far from the solution, the strategy may take longer to converge.

The admittance matrix is used to write equations for currents entering a power system.

Equation (3.56) is expressed in a polar form, in which j includes bus i

$Ii = \sum_{j=1}^{n} |Y_{ij}| |V_j| < \theta_{ij} + \delta_j$ (3.60)

The real and reactive power at bus i is

$P_i - jQ_i = V_i * I_i$ (3.61)

Substituting for Ii in Equation (3.56) from Equation (3.57)

$P_i - jQ_i = |V_i| < -\delta_i \sum_{j=1}^{n} | Y_{ij} | \, | | V_j | \, | < \delta_{ij} + \delta_j$ (3.6

The real and imaginary parts are divided

$$P_i = \sum n_j = 1 \; |V_i||V_j||Y_{ij}| \; \cos(\theta_{ij} - \delta_i + \delta_j) \quad (3.62)$$

$$Q_i = \sum n_j = 1 \; |V_i||V_j||Y_{ij}| \; \sin(\theta_{ij} - \delta_i + \delta_j) \quad (3.63)$$

The above Equation (3.62) and (3.63) establish a set of non-linear algebraic equations in terms of |V| in per unit and δ in radians. Equation (3.62) and 3.63) are prolonged in Taylor's series about the initial estimation and ignoring all higher order terms, the following set of linear equations are obtained.

$$\begin{bmatrix} \Delta P_2^{(K)} \\ \cdot \\ \cdot \\ \cdot \\ \Delta P_n^{(K)} \\ \Delta Q_2^{(K)} \\ \cdot \\ \cdot \\ \cdot \\ \Delta Q_n^{(K)} \end{bmatrix} = \begin{bmatrix} \frac{\Delta P_2^{(K)}}{\partial \delta_2} & \cdots & \frac{\Delta P_2^{(K)}}{\partial \delta_n} & \frac{\Delta P_2^{(K)}}{\partial |V_2|} & \cdots & \frac{\Delta P_2^{(K)}}{\partial |V_n|} \\ \vdots & \ddots & \vdots & \vdots & \ddots & \vdots \\ \frac{\Delta P_n^{(K)}}{\partial \delta_2} & \cdots & \frac{\Delta P_n^{(K)}}{\partial \delta_2} & \frac{\Delta P_n^{(K)}}{\partial |V_2|} & \cdots & \frac{\Delta P_n^{(K)}}{\partial |V_n|} \\ \frac{\Delta Q_2^{(K)}}{\partial \delta_2} & \cdots & \frac{\Delta Q_2^{(K)}}{\partial \delta_n} & \frac{\Delta Q_2^{(K)}}{\partial |V_2|} & \cdots & \frac{\Delta Q_2^{(K)}}{\partial |V_n|} \\ \vdots & \ddots & \vdots & \vdots & \ddots & \vdots \\ \frac{\Delta Q_n^{(K)}}{\partial \delta_2} & \cdots & \frac{\Delta Q_n^{(K)}}{\partial \delta_n} & \frac{\Delta Q_n^{(K)}}{\partial |V_2|} & \cdots & \frac{\Delta Q_n^{(K)}}{\partial |V_n|} \end{bmatrix} \begin{bmatrix} \Delta \delta_2^{(K)} \\ \cdot \\ \cdot \\ \cdot \\ \Delta \delta_n^{(K)} \\ \Delta \left| \frac{V_2^k}{V} \right| \\ \cdot \\ \cdot \\ \cdot \\ \Delta \left| \frac{V_n^k}{V} \right| \end{bmatrix} \quad (3.64)$$

Because the slack bus variable voltage magnitude and angle are already known, they are not included in the preceding equation. After partial derivatives of Equations (3.62) and (3.63) are expressed, the element of the Jacobian matrix is obtained, which establishes a linearized relationship between tiny changes in voltage magnitude and voltage angle. The following is a matrix representation of the equation:

$$\begin{vmatrix} \Delta P \\ \Delta Q \end{vmatrix} = \begin{vmatrix} J_1 & J_3 \\ J_2 & J_4 \end{vmatrix} \begin{vmatrix} \Delta \delta \\ \Delta \frac{|V|}{V} \end{vmatrix} \quad (3.65)$$

Where J_1, J_2, J_3, J_4 are the elements of the Jacobian matrix and

$$J1 = \frac{\partial P}{\partial \delta} = J2 = \frac{\partial P}{\partial V} = \quad J3 = \frac{\partial Q}{\partial \delta} = J4 \quad = \frac{\partial Q}{\partial V} \quad (3.66)$$

The difference between the schedule and calculated values known as power residuals for the terms $\Delta Pi\,(k)$ and $\Delta Qi\,(k)$ is represented as:

$$\Delta Pi\,(k) = Pisch - Pi\,(k);\ i=2,\ n-1 \quad (3.77)$$

$\Delta Qi\ (k) = Qisch - Qi\ (k)$; i=n+1, .n-1-m (3.78)

The new estimates for bus voltage are

$\delta\ (k+1) = \delta\ (ik) + \Delta\delta\ (ik)$ (3.79)

$|V\ (k+1)| = |Vi\ (k)| + \Delta|Vi\ (k)|$ (3.80)

3.5.2 Iterative Algorithm

The iterative algorithm for the solution of the load flow problem by the NR method is as follows:

1. With voltage and angle (usually δ=zero at slack bus, assume ∣V∣, δ at all PQ buses and δ at all PV buses. In the absence of any other information flat voltage start is recommended.

2. Compute ΔPi (for PV and PQ buses) and ΔQi (for all PQ buses) from Eqs. (3.77) and (3.78). If all the values are less than the prescribed tolerance, stop the iterations, calculate P1 and Q1 and print the entire solution including line flows

3. If the convergence criterion is not satisfied, evaluate elements of the Jacobian using Eq. (3.76).

4. Solve Eq. (3.75) for corrections of voltage angles and magnitudes.

5. Update voltage angles and magnitudes by adding the corresponding changes to the previous values and return to step 2.

Note: 1. In step 2, if there are limits on the controllable Q sources at PV buses, Q is computed each time and if it violates the limits, it is made equal to the limiting value and the corresponding PV bus is made a PQ bus in that iteration. If in the subsequent computation, Q does come within the prescribed limits, the bus is switched back to a PV bus. 2. If there are limits on the voltage of a PQ bus and if any of these limits is violated, the corresponding PQ bus is made a PV bus in that iteration with voltage fixed at the limiting value.

The flowchart of the Newton-Raphson load flow method is shown in Figure 3.5 [35]

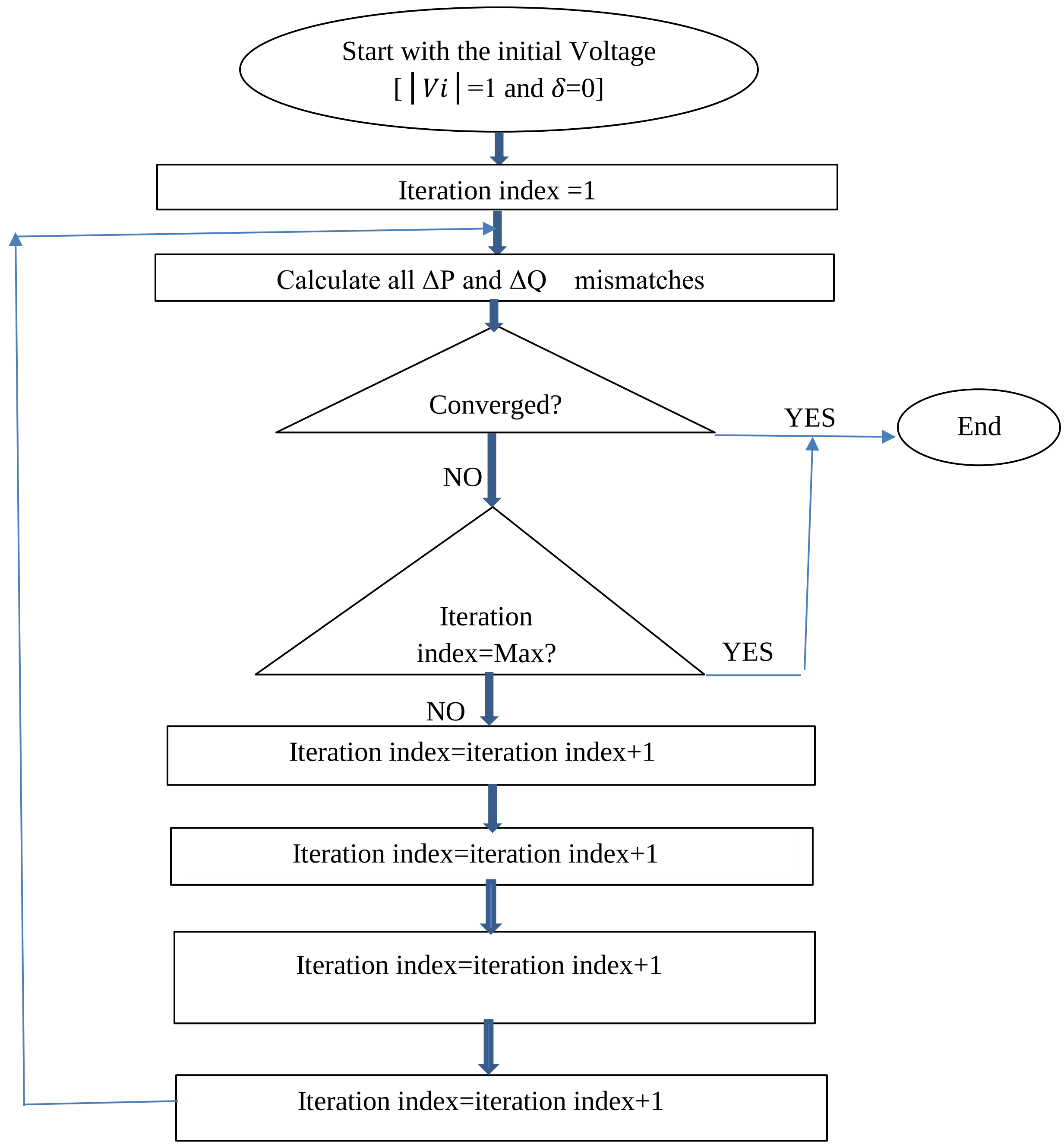

A single-phase model is utilized to solve a power flow problem since the system is believed to be operating under balanced conditions. Each bus is related with four different quantities. Voltage magnitude $|V|$, phase angle δ, real power P, and reactive power Q are the four variables. The system buses are divided into three categories.

Slack bus one bus, referred to as the slack or swing bus, is used as a reference for determining the magnitude and phase angle of the voltage. This bus compensates for the mismatch between scheduled loads and generated power induced by network losses.

Load buses The active and reactive powers are given on these buses. The magnitude of the bus voltages as well as their phase angle are unknown. P-Q buses are the name of these buses.

P-V buses these buses are the generator buses. They are also known as voltage-controlled buses. The real power and voltage magnitude are specified on these buses. It is necessary to establish the phase angles of the voltages as well as the reactive power. There are additional constraints on the amount of reactive power that can be used. These buses are called regulated buses.

3.6 Power Flow Model of Unified Power Flow Controller

The UPFC consists of two identical inverters these are parallel inverter and series inverter, which are connected in parallel and series to power systems through corresponding power transformers. The UPFC is connected between the buses i and j through the series and parallel power transformers as shown in fig (3.10 Voltage source model of UPFC). The parallel inverter can operates either voltage controller or constant reactive power source. It injects constant positive or negative reactive power at i^{th} bus reactive power (Q_i) and regulates the voltage of the bus. The series inverter independently controls the active power (P_j) and reactive power $(Q_j)$of the j^{th} bus at associated settings, which distinguishes the UPFC from the STATCOM and SSSC. Also the series inverter is used to regulate the difference between the i^{th} bus voltage V_i and j^{th} bus voltage V_j bus. By using the load flow solution, the real and reactive power at the bus i and j is calculated. The importance of the power injection representation is that the symmetric characteristics of admittance matrix will not be destroyed [16].

3.6.1 Problem Formulation

Reducing active and reactive losses and enhancing the voltage profile are among the goals of the study. When creating the objective function of the ideal placement of a unified power flow controller, a number of optimization factors can be taken into account. In this study, a multi-objective function that minimizes active power loss and voltage variation is suggested for determining the ideal location and size of UPFC. A transmission line's performance has been calculated utilizing the number of objective functions, UPFC sizes, and placement planning.

$Min F_t$ (A, C) (3.81)

Subject To:

G_t (A, C) = 0 (3.82)

H_t (A, C) ≤ 0 (3.83)

If A goes out of bounds, C can be adjusted so that A can be within limits again. Line losses are considered for optimization since losses can be controlled by varying voltages at different nodes. Where

F_t (A, C): describes the objective function to be reduced and optimized;

G_t (A, C): describes the equality constraints focused on active and reactive power according to the balance equations.

H_t (A, C): describes the inequality constraints focused on UPFC parameter ranges, reactive power ranges, and bus voltage ranges.

A describes the group of states of the power system containing voltage magnitude and phase angles.

C: describes the group of controlling variables to be optimized to become the output of the process. In this case, minimization of real power losses, voltage drops, and cost losses is considered the objective function, and it can be computed mathematically as follows:

3.6.1.1 1Minimize Active Power Losses:

The active power losses in the distribution system should be minimized as much as possible for reliable power transfer.

$F_1 = min \sum_{i=1}^{nb} R_I I_I^2$ (3.84)

$where, F_1$ is objective function representing active power loss, R_I is the line resistance i, I_I, is the current of line i and nb is the number of system branches.

$Q_{Loss} = \sum_{i=1}^{nb} X_I I_I^2$ (3.85)

$where,$ is the reactive power loss, X_I is the reactance of line i.

3.6.1.2 Voltage Profile enhancement

As mentioned in preceding section, UPFC can compensate reactive power and improve the voltage profile. The objective function for enhancing voltage profile is as expressed follows

F_2 =min $\sum_{i=1}^{nb}(V_{nomi} - V_i)^2$ (3.86)

$where\ F_2$ is the objective function for voltage profile improvement, $V_{nomi}$is the nominal voltage of the system which is equal to 1 p.u, V_i is the voltage of the i^{th} bus.

3.6.1.3 System Constraint

The formulated multi-objective function, declared above is minimized subject to various operational constraints.

Voltage Limit:-

Voltage constraints are dependent of reactive power injection to the generator bus. According IEEE the voltage limits are usually kept within a predefined range of ±5%. This thesis work bounds the upper and lower voltage limits equal to 1.05 p.u. and 0.95 p.u., respectively. Therefore, at any bus i, the following inequality voltage constraint holds, the system voltage in all buses should be in an acceptable range.

$V_{min} \leq V_i \leq V_{max}$ (3.87)

Where $V_{min} = 0.95\ p.u,$ V_{max} = 1.05 p.u

Reactive Power Compensation: - To get the optimum solution, the size of the distribution static compensator should not be either minimal or too large in relation to the load value. The reactive power injected by UPFC to the system is limited by lower and upper bounds as given in following. the total reactive power injection Qi is not to exceed the total reactive power demand Qi in the distribution system.

$Q_{min} \leq Q_{UPFC} \leq Q_{max}$ (3.88)

Active power losses constraint

The equality constraints represent the power flow equations expressed as:

$\sum_{i=1}^{nb} P_{Gi} - P_{Di} = P_L$ (3.89)

$\sum_{i=1}^{nb} Q_{Gi} - Q_{Di} = Q_L$ (3.90)

P_{Gi} and Q_{Gi} are the total active and reactive power generation at bus i respectively, $P_{Di}$and Q_{Di} are the total active and reactive power demand at bus k respectively, $P_L$and $Q_L$are the total active and reactive power losses.

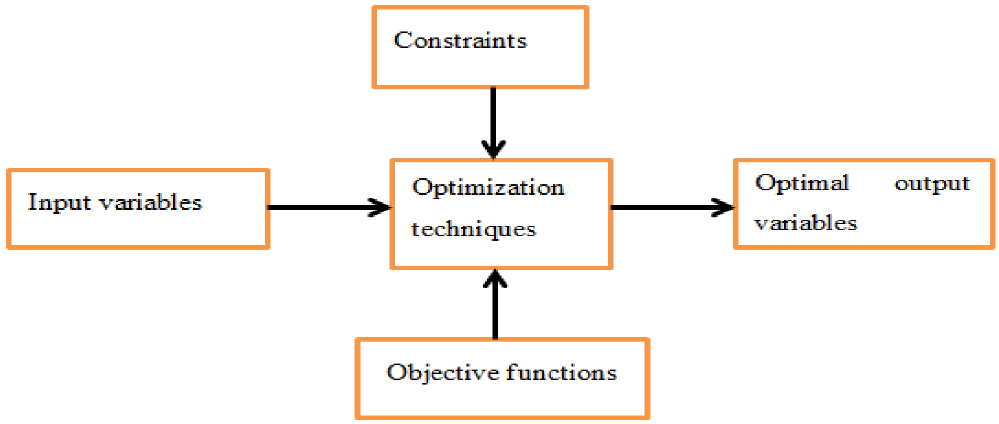

Figure3. 17 problem formulation expression

System Parameters of Unified Power Flow Controller

3.7 Controller system of UPFC

The operation of the UPFC in the automatic control mode which is discussed sub section 3.3 in this chapter, and also to use the UPFC so as to enhance power system stability and to improve voltage profile two control designs need to be performed. The first and basic control design, which is also referred to as the UPFC basic control design, involves simultaneous control of

(i) real and reactive power flow on the transmission line,

(ii) sending bus voltage magnitude, and

(iii) DC voltage magnitude.

The second control design, referred to as the damping controller design, is a supplementary control loop that is designed to improve transient stability of the entire electric power system. The control design of UPFC consists of series control scheme, whose objective is to control of real and reactive power flow on the line, and a shunt control scheme, to control the sending bus voltage magnitude and the DC voltage magnitude [6].

3.7.1 Series control scheme

Series control scheme consists of two control loops, one for the tracking of the real power flow at the receiving bus of the line, and the second performs the same task for the reactive power flow. Specifically, the objective is to track these real and reactive power flows following step changes and eliminate steady-state tracking errors. This is obtained by the appropriate selection of the voltage drop between the sending and the receiving buses, which is denoted by V_{PQ}. This voltage can be decomposed into the following two quantities PQ which affect the tracked powers, namely:

V_P = voltage component orthogonal to the sending bus voltage that affects primarily the real power flow on the transmission line.

V_Q = component in phase with the sending bus voltage that affects mainly the reactive power flow on the transmission line.

Both voltages, V_P and V_Q, are obtained by designing classic PI (proportional-integral) controllers. The integral controller will guarantee error free steady state control of the real and reactive line power flows.

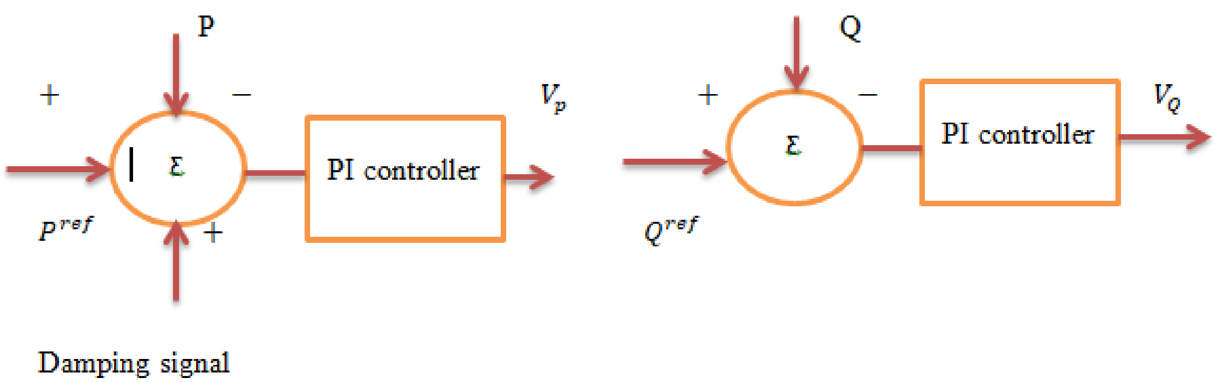

Figure3. 18 Series control scheme

3.7.2 Shunt control scheme

This control scheme also has two loops that are designed to maintain the magnitude of the sending bus voltage and the DC link voltage at their pre-specified values. The magnitude of the injected shunt voltage, affects the reactive power flow in the shunt branch, which in turn affects the sending bus voltage magnitude. The angle between the sending bus voltage and the injected shunt voltage, affects the real power flow in the shunt brunch. It can be used to control the power flow to the DC link and therefore the DC link voltage [6].

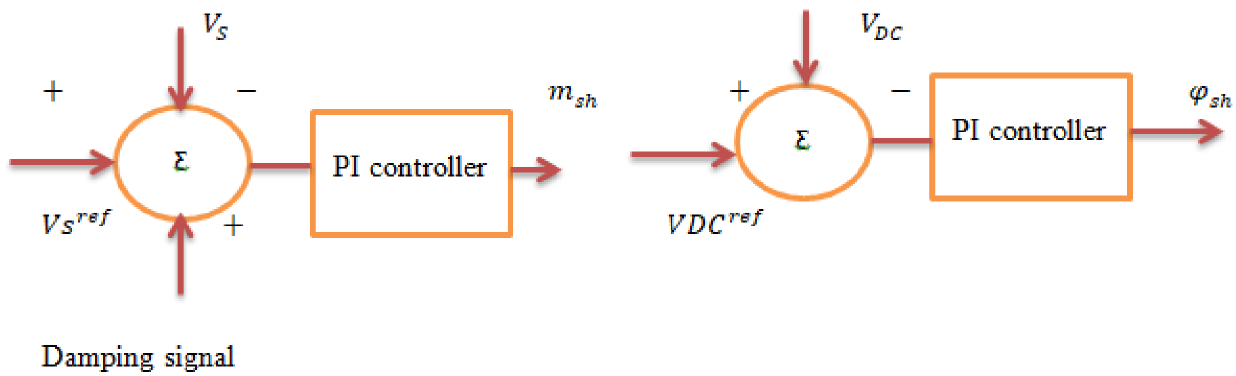

Figure3. 19Fig Shunt control scheme

3.8 Damping Controller Design

Low-frequency oscillations are a common occurrence in power systems, often triggered by disturbances such as changes in loading conditions or the loss of a transmission line or generator unit. These oscillations need to be controlled effectively to ensure system stability. Several control devices, such as power system stabilizers, are employed to improve power system stability. It has been shown that these oscillations can be damped by introducing a supplementary signal to the system. This can be achieved by modulating the active power flow reference signal on the series converter side or by adjusting the voltage magnitude reference signal on the shunt converter side, both of which are based on real power flow along the transmission line. Historically, damping controllers have used a lead-lag type transfer function, as illustrated in the figure below [6]. The damping controller designed in this research, however, is based on fuzzy logic. Below, I provide a brief introduction to fuzzy set theory, the fundamentals of fuzzy control design, and its application to the design of the UPFC damping controller.

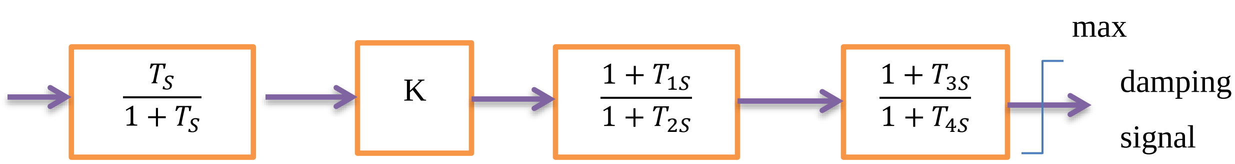

Figure3. 20 Lead –lag controller structure

3.8.1 Introduction

Fuzzy logic control is based on fuzzy set theory and offers significant advantages in power system control. One of the key benefits is that it does not require a mathematical model of the system. Instead, it uses rule-based controllers that are formulated in an "if-then" format. The "if" part is called the condition, while the "then" part is the conclusion. Modern energy systems are large, complex, geographically distributed, and highly nonlinear. Additionally, the operating conditions and topology of the power grid are constantly changing, and interruptions can be unpredictable. Conventional controllers based on linear system models struggle to address power system stability issues effectively due to these uncertainties. As a result, the fuzzy logic control approach has become a significant field of artificial intelligence that complements traditional control methods. A fuzzy logic controller is considered an intelligent controller because it allows for easy integration of human knowledge and governing laws. Another advantage is that fuzzy logic controllers are nonlinear and can adapt to changes in system topology, parameters, and operating conditions. The fuzzy rules may incorporate multiple variables in both the condition and conclusion parts of the rules. This flexibility makes fuzzy logic controllers applicable to both nonlinear multi-input-multi-output (MIMO) and single-input-single-output (SISO) problems [6].

3.8.1.1 Structure of a Fuzzy Controller

A fuzzy controller structure which is shown in Fig below is placed between preprocessing and post-processing blocks (input and output).

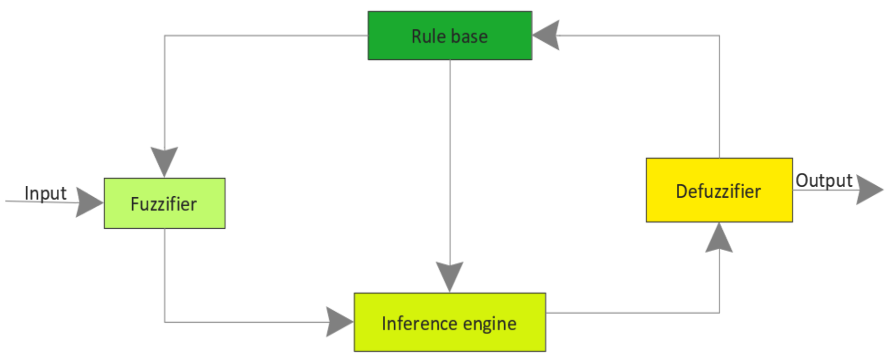

Figure3. 21 Structure of a Fuzzy Controller

The preprocessing block conditions inputs, basically crisp measurements, before they enter the controller. Choosing of the appropriate input and output signals of the controller in the fuzzy controller is the first step of the design. The second step is to choose linguistic variables that will describe all input and output variables. Third step is to define membership functions for fuzzy sets. Membership functions can be of different shape i.e. triangular, trapezoidal, Gaussian functions etc. Fourth step is to define fuzzy rules.

Fuzzification

Fuzzy logic is a technique used to convert a crisp numerical value into a fuzzy value, represented as a linguistic variable. This process is guided by a knowledge-based membership function that maps the input variable into the fuzzy domain. Unlike traditional approaches that rely on precise numerical values, fuzzy logic uses linguistic terms to describe the input.

Fuzzy Interference

The fuzzy interpolation process uses fuzzy logic to map the supplied input to the output. Fuzzy sets (and corresponding rules) enable this mapping, allowing for nonlinear outputs. The range and domain of this mapping are represented as fuzzy sets or points within multidimensional spaces. Fuzzy interpolation systems have been successfully applied across various fields, including automatic control, data classification, decision analysis, expert systems, and computer vision. A fuzzy inference system, which is also known by several names such as a fuzzy rule-based system, fuzzy associative memory, fuzzy expert system, fuzzy logic controller, fuzzy model, or simply a fuzzy system, is recognized for its wide range of functions.

Defuzzification

It is used to convert the fuzzy value (linguistic value) into the crisp value (numerical value) from a mathematical calculation. It uses various defuzzification methods that have the minimum error and easily fit in the system. For the best result, the output membership function is compared with different process cycles from the most significant point.

Mapping Expert Knowledge to Fuzzy Rules

There are two inputs to the FLC. One is the control error $e(k)$, which is the difference between the desired (reference) value and the measured value x (t), and the other is the rate of change in the control error $\Delta e(k)$. These two inputs, defined in equation below, are first fuzzified and converted to fuzzy membership values that are used in the rule base in order to execute the related rules so that an output can be generated.

$e(k) = x*(t) - x(t)$ ……………………………………………………………….3.91

$\Delta e(k) = e(k) - e(k-1)$ ……………………………………………………………..3.92

Where;

- ✓ $x*(t)$ The desired (reference) value
- ✓ $x(t)$ Measured value
- ✓ $x(t)$ Represents for speed, Voltage and reactive current

The fuzzy rule base, which may also be called as the fuzzy decision table, is the engine mapping the two crisp inputs, e (k) and Δe (k) to the fuzzy output space defined on the universe of $\Delta(k)$. In order to intuitively generate the set of rules for the FIS, the system response is analyzed thoroughly first. The time response of the control error (k) for a step input can be represented by the generalized step response error of a second-order system. This error signal may have a damped or an oscillatory response with a decaying exponential component. The latter one is considered for constructing the rule table since it includes overshoot effects, leading the rule base to represent more generalized cases.

Table below shows 49 rules

$e(k)$	Δe(k)						
	NB	NM	NS	ZE	PS	PM	PB
PB	KV	IS	IM	IB	IB	IB	IB
PM	DS	KV	IS	IM	IB	IB	IB
PS	DM	DS	KV	IS	IM	IB	IB
ZE	DB	DM	DS	KV	IS	IM	IB
NS	DB	DB	DM	DS	KV	IS	IM
NM	DB	DB	DB	DM	DS	KV	IS
NB	DB	DB	DB	DB	DM	DS	KV

From the general conventional control, the error is given by $e(k) = x*(t) - x(t)$and assuming a constant set point one can arrive at $\frac{de(k)}{dt} = -\frac{dx(t)}{dt}$

Where e (k) = error signal

$x*(t)$ = desired output signal

x(t)= actual output signal

- $e(k)$= negative, which means “the UPFC output power”, is greater than the reference power, so the UPFC needs to decrease its output.

- e(k)= positive, Means "the UPFC output power" is less than the reference power, so the UPFC needs to increase output power until it reaches the desired value or until error is zero.
- $\frac{dx(t)}{dt}$ = negative, means power is decreasing this implies $\frac{de(k)}{dt}$= positive. Therefore, a positive change in the error rate indicates the power is decreasing.
- $\frac{dx(t)}{dt}$= positive, means output power is increasing this means $\frac{de(k)}{dt}$= negative. Therefore, a negative change in the error rate indicates the power is increasing.

3.8.1.2 Adaptive Neuro-Fuzzy Inference System (ANFIS) controller

ANFIS is a sort of adaptive control that uses a combination of fuzzy logic and neural networks to learn the dynamics of the system and provide control signals. Reactive power output can be modified by UPFC using ANFIS based on current and voltage measurements taken in real-time. The benefits of fuzzy logic and neural networks are combined in this particular sort of artificial neural network. The input layer, fuzzy layer, normalization layer, rule layer, and output layer are the five layers that make up the ANFIS architecture as shown in figure below. The input layer receives the input variables, which are subsequently sent to the fuzzy layer, where fuzzy sets are defined and evaluated and membership functions are applied. The input values are scaled in the normalization layer to a common range, and the fuzzy sets are combined in the rules layer to produce rules. The output layer produces the output by applying a weighted sum of the rules.

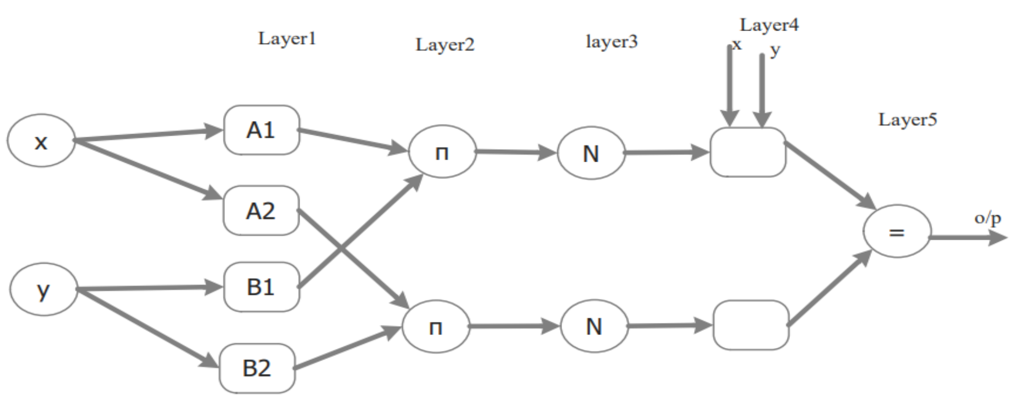

Figure3. 22 Internal Structure of ANFIS

ANFIS uses a hybrid-learning algorithm that combines gradient descent and least squares methods to adjust the parameters of the membership functions and rule weights. This allows

ANFIS to learn from data and adapt to changes in input-output relationships. ANFIS has been successfully applied to a variety of problems, including prediction, classification, and control [].

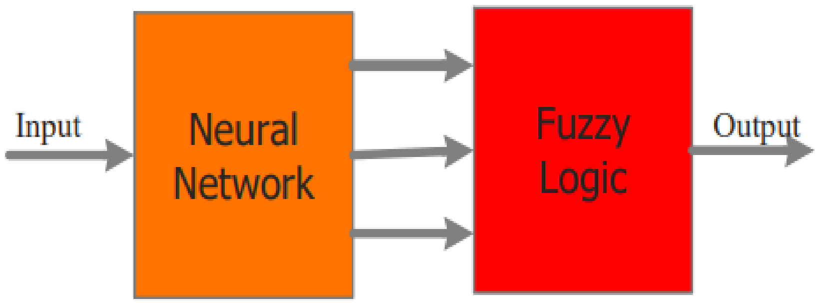

Figure3. 23 Structure of ANFIS

3.9 Grey Wolf Optimizer (GWO)

The Grey Wolf Optimizer (GWO) is inspired by the social hierarchy and group hunting behavior of grey wolves in nature. It is capable of optimizing problems with multiple variables, often yielding better or highly competitive results compared to other popular algorithms such as Genetic Algorithms (GA) and Particle Swarm Optimization (PSO) [25]. Proposed by Mirjalili et al. in 2014, the GWO is a novel optimization technique designed to address problems across various sectors, including engineering and science. The algorithm draws on the social structure and hunting strategies of grey wolves. In GWO, a population of grey wolves searches for the best solution to a problem. Each wolf represents a potential solution, and its fitness is evaluated based on its position in the search space. The algorithm progresses through iterations, with each iteration consisting of three key steps: The three best wolves in the population are designated as alpha, beta, and delta wolves. The alpha wolf is the best solution, the beta wolf is the second best, and the delta wolf is the third best. These wolves guide the search, helping the other wolves converge toward the optimal solution. GWO has proven effective in solving a broad range of optimization problems, such as engineering design, data clustering, feature selection, and image processing. It has also demonstrated superior performance compared to other optimization algorithms like Particle Swarm Optimization and Genetic Algorithms, particularly in terms of convergence speed and solution quality. Grey wolves, known as top predators, live and hunt in packs, which is reflected in the GWO's social hierarchy. The algorithm models four types of wolves: alpha, beta, delta, and omega. The fittest solution is considered the alpha (α), while the second and third best solutions are termed beta and delta, respectively. The remaining solutions are considered omega wolves. GWO's optimization process is based on four key components: hunting, pursuing and searching for prey, encircling prey, and attacking prey. In addition to the social hierarchy, the group hunting behavior of grey wolves plays a significant role in the algorithm's structure. According to [27], the basic phases of grey wolf hunting include:

- Tracking, chasing, and approaching the prey
- Pursuing, encircling, and harassing the prey until it stops moving
- Attack towards the prey

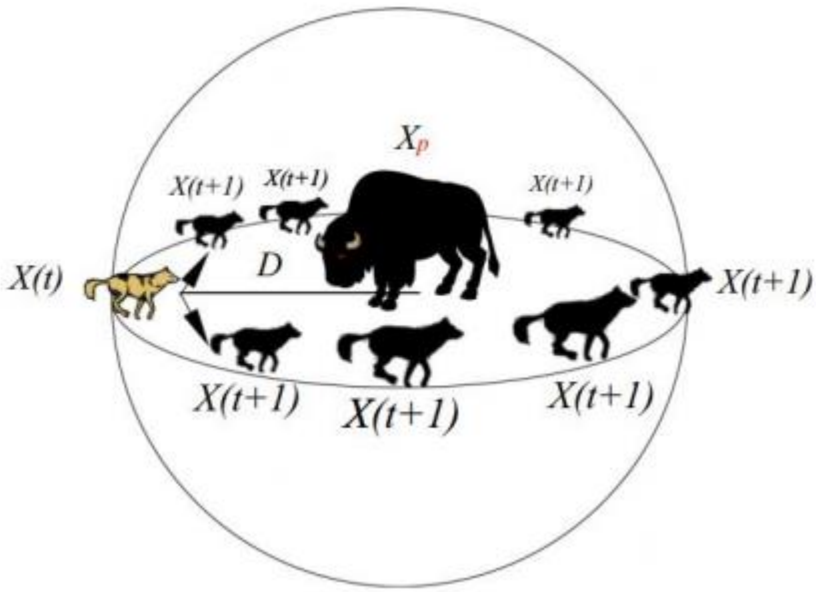

Figure3. 24 wolfs position updating

3.9.1. Mathematical model and algorithm

In this section the mathematical models of the social hierarchy, tracking, encircling, and attacking prey are explained well.

3.9.2. Social hierarchy

In order to mathematically model the social hierarchy of wolves when designing GWO, we consider the fittest solution as the alpha (α). Consequently, the second and third best solutions are named beta (β) and delta (δ) respectively. The rest of the candidate solutions are assumed to be omega (ω). In the GWO algorithm the hunting (optimization) is guided by α, β and δ the ω wolves follow these three wolves.

3.9.3 Encircling prey

Grey wolves surround their victim during hunting, as mentioned above. The following equations are used to model encircling behavior mathematically.

$$\vec{D} = |\overrightarrow{C.}\vec{X}_p(t) - \vec{X}(t)| \quad (3.93)$$

$$\vec{X}(t+1) = \vec{X}_p(t) - \overrightarrow{(A.}\vec{D}) \quad (3.94)$$

Where t indicates the current iteration $\vec{A}$ and $\vec{C}$ are coefficient vectors $\vec{X}_p$ is the position vector of the prey, and $\vec{X}$ indicates the position vector of a grey wolf. The vectors are calculated as follows:-

$$\vec{A} = 2\,\vec{a}.\vec{r}_1 - \vec{a} \quad (3.95)$$

$$\vec{C} = 2.\vec{r}_2 \quad (3.96)$$

Where components $\vec{a}$ of are linearly decreased from 2 to 0 over the course of iterations $\vec{r}_1$and $\vec{r}_2$, are random vectors in [0, 1].

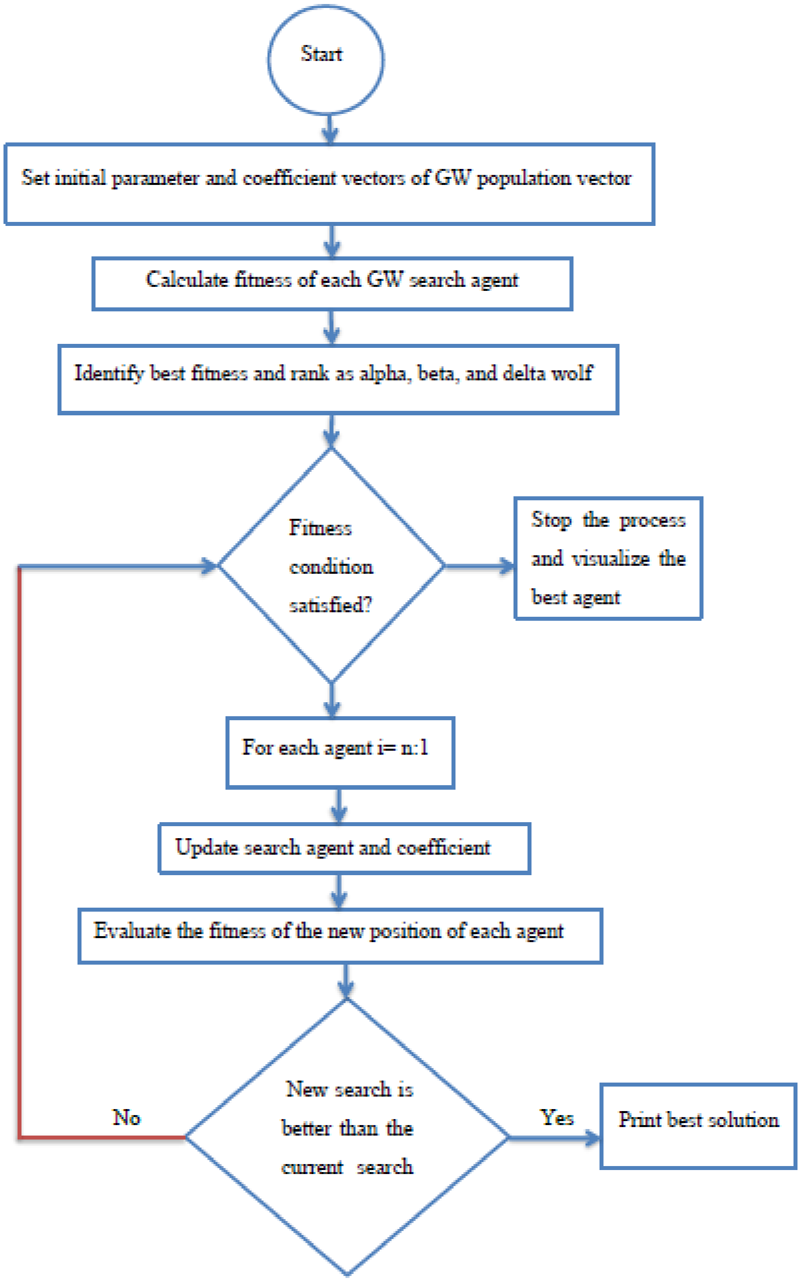

Figure3. 25 grey wolf optimizer algorithm

3.9.4 the most important parameters to be considered when using Grey Wolf Optimizer

Several parameters can influence the performance of the Grey Wolf Optimizer (GWO) algorithm, and the selection of these parameters plays a crucial role in determining the quality of the solutions produced. The social hierarchy concept in GWO helps grade the solutions and retain the best ones for the current iteration. The encircling mechanism defines the solution and its neighborhood in a 2D circle, which can be extended to a 3D hyper sphere in higher dimensions [10].

When applying GWO, some of the most important factors to consider include:

i. Population Size: this establishes how many wolves are present in the search region. Although a larger population size may result in more diverse solutions, it may also lengthen the computation time.

ii. Maximum Number of Iterations: The search process's duration is determined by the maximum number of iterations. The quality of the solutions can be enhanced by more iteration.

iii. Search Range: The range of values that the decision variables can take is determined by the search range. Although a larger search range can yield more diverse results, it can also result in longer processing times.

iv. Alpha, Beta, and Delta variables: the alpha, beta, and delta wolves' positions are established by these variables, which direct the search.

v. Crossover Rate: The likelihood of two wolves sharing information during a search is determined by the crossover rate.

vi. Fitness Function: The objective function under optimization is the fitness function. The GWO algorithm's performance may be significantly impacted by the fitness function's quality.

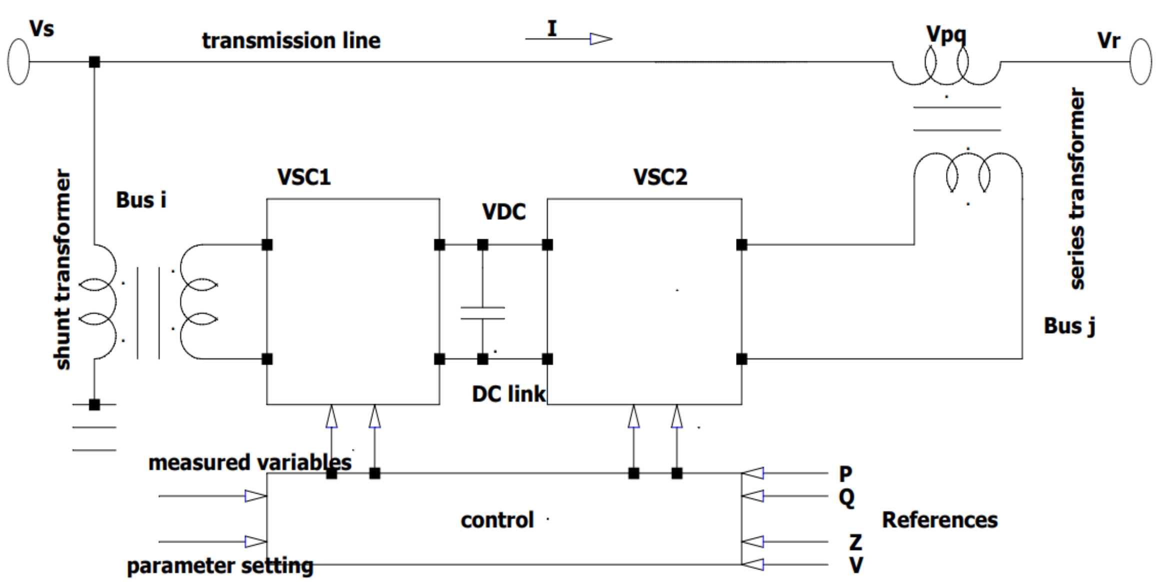

Figure3. 26 over all circuit diagram of thesis with allocation of UPFC.

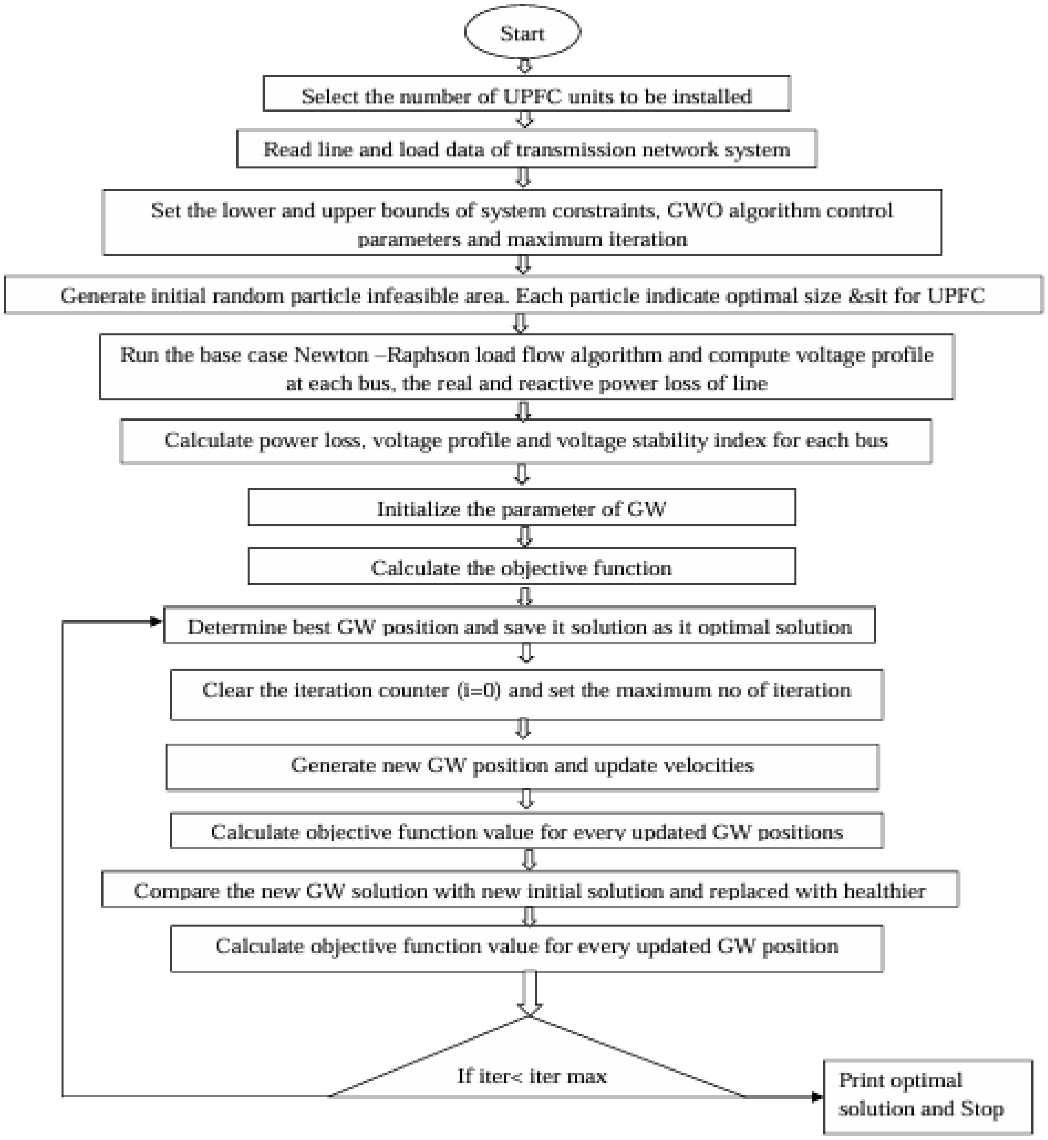

Figure 3.27 over all flowchart of the thesis with allocation of UPFC

CHAPTER FOUR
RESULT AND ANALYSIS

4.1 Introduction

This section presents the calculated results and provides an explanation of them. The Ethiopian network (from the GERD to the HOLETA 500/400 kV transmission line) is used to evaluate the effectiveness of the Grey Wolf Optimization-based Unified Power Flow Controller (UPFC). The objective of this research is to utilize an intelligent controller-based UPFC device to reduce power loss, enhance system reliability, and improve power system stability. The GERD-DEDSA-HOLETA-HOLETA 500/400 kV network is simulated using MATLAB. The simulation explores the impact of positioning the UPFC at different grid locations to assess variations in voltage stability and improvements in power transfer across the grid. This chapter summarizes the findings from the simulations conducted in MATLAB. In the current system, the load flow of the transmission network is analyzed, and the voltage profile and power loss are determined. After establishing the voltage profile and power loss, the UPFC compensation method is thoroughly examined. The voltage stability index is used to identify critical buses for UPFC placement. Potential buses are selected using Grey Wolf Optimization (GWO) within the MATLAB environment. To find the optimal UPFC reactive power (KVAR), these candidate buses, along with various static compensator values, are used as inputs. The first bus is considered the slack bus, and other buses within the range are assessed for UPFC placement of the specified size. The system's voltage profile index is evaluated with a reference voltage of 1. The overall objective function is then determined by applying the Grey Wolf Optimization technique. The UPFC devices are controlled by a fuzzy logic controller under various fault conditions. By comparing system parameters, such as voltage and phase angle, with the reference values, the fuzzy logic controller generates triggering pulses for the UPFC's voltage source converter. The proposed model is simulated in a MATLAB environment. The simulation results are assessed using IEEE standards and compared to existing models to evaluate the significant impact of the proposed model.

4.2. Voltage profile comparison, (from GERD to HOLETA 500/400 kV transmission line network)

Table 4.1 presents the voltage magnitude for the base case (without the UPFC). The table indicates that the lowest voltage magnitude is 0.872 pu. With the exception of the slack bus, all other buses fall below the 0.95 pu threshold, exceeding the acceptable limits of the base case. This suggests the need for upgrades to the buses that have surpassed these constraint limits.

The ideal size and location of the UPFC to be added to the test network were determined using Grey Wolf Optimization, following the power flow study without the UPFC. The results showed that the optimal size of the UPFC was 757.5 KVAR on average. After installing the UPFC, the voltage magnitude (pu) increased. The voltage magnitude for each bus after the UPFC installation is presented in Table 4.1. The minimum voltage magnitude with the UPFC implementation is 0.966 pu, as shown in the table. Compared to the base-case values, Table 4.1 reveals that the Grey Wolf Optimization technique successfully brought all buses within the acceptable voltage range ($0.95 \leq 1.05$ pu), with no buses

MATLAB R2016a software was used to simulate the Newton –Raphson Method load flow algorithm both for the base case and with the integration of the UPFC, using data from the GERD to HOLETA 500/400 kV transmission line. The Newton –Raphson Method load flow method determines the voltage profile for each bus, first without UPFC integration (base case), and then after UPFC integration. In the base case, the minimum voltage of 0.872 pu falls below the IEEE standard minimum voltage range for transmission systems, which is also applicable to Ethiopian Electric Power (EEP). While the remaining voltage profiles in the base case meet IEEE standards and are generally acceptable, improvements are still necessary to increase power flow capacity. To enhance the voltage profile, the Grey Wolf Optimizer (GWO) algorithm was employed to determine the optimal size and location of the UPFC. According to GWO, the UPFC is placed at bus 3 with a capacity of 757.5 KVAR. After UPFC integration, reactive power compensation is achieved, and all buses meet the IEEE standards mandated by EEP. The voltage profile of the distribution system is significantly improved. MATLAB results show that the minimum voltage after UPFC integration is 0.966 pu, and the maximum voltage reaches 1.00 pu. As a result, the entire bus voltage profile is brought within the acceptable range ($0.95 \leq 1.05$ pu), and the minimum voltage has increased from 0.872 pu to 0.966 pu an improvement over the base case. Following reactive power compensation, all buses now meet the system's standard voltage profile. These results are further illustrated in both tabular and graphical forms below.

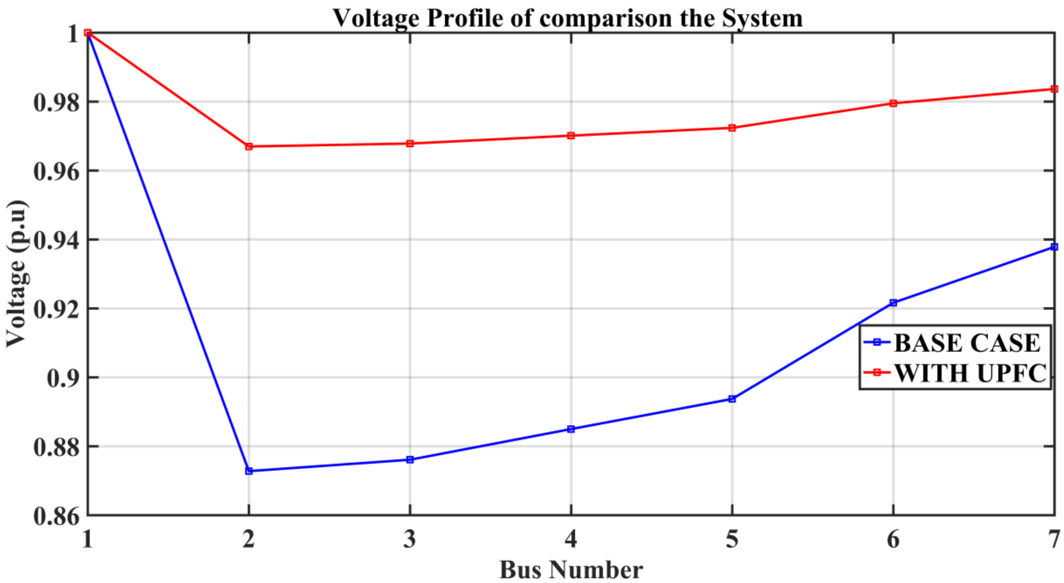

Figure4. 1 voltage profile comparison

Table4. 1voltage profile comparison

Bus no	Voltage profile base case (without UPFC)	Voltage profile with UPFC
1	1.000	1.000
2	0.873	0.967
3	0.876	0.968
4	0.885	0.970
5	0.894	0.9724
6	0.922	0.979
7	0.937	0.984

4.3 Reactive power loss comparison, (from GERD to HOLETA 500/400 kv transmission line network)

The Newton –Raphson Method sweep technique is applied to analyze the power flow in the base case of the GERD to HOLETA 500/400 kV transmission line network, with the results shown in Table 2.2 below. The maximum reactive power loss of 299.7 KVAR occurs at the last bus, while the total reactive power loss for the network is 468.9 KVAR. Figure 4.2 illustrates the reactive power loss at each bus in the base case of the GERD to HOLETA 500/400 kV transmission line network.

After integrating the UPFC into the GERD to HOLETA 500/400 kV transmission line network, the last bus experiences the highest reactive power loss of 21.7 KVAR. The total reactive power loss for the network is calculated to be 33.6 KVAR. Figure 4.2 shows the reactive power losses for each bus in the system with UPFC integration.

Reactive power and operational voltage are closely related in a power system. Insufficient reactive power can cause the voltage to drop to zero, while adequate reactive power helps enhance the system's voltage profile. Therefore, minimizing reactive power loss is crucial for maintaining system stability. The Newton –Raphson Method load flow algorithm, implemented in MATLAB R2016a software, was used to calculate the reactive power loss in the GERD to HOLETA 500/400 kV transmission line network. According to the simulation results, the base case reactive power loss in this network is 468.9 KVAR. To ensure system stability, it is essential to minimize power losses in the transmission system. To achieve this, the UPFC must be used to significantly reduce power loss. The optimal size and location of the UPFC, determined through the Grey Wolf Optimization (GWO) method, were found to be 757.5 KVAR and bus 3, respectively. When the UPFC was installed at the designated bus, the reactive power loss decreased from 468.9 KVAR to 33.6 KVAR. The reactive power losses for each bus, both for the base case and with UPFC, are presented in Table 4.2.

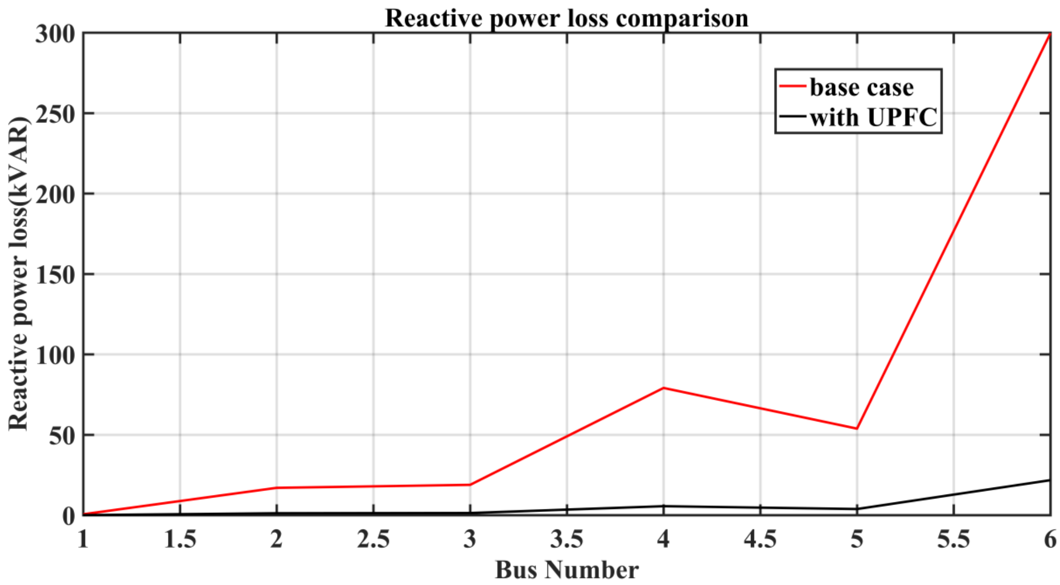

Figure4. 2 reactive power loss comparison

Table4. 2 reactive power loss comparison

Bus No	Reactive Power Loss base case (KVAr)	Reactive Power Loss with UPFC (KVAr)
1	0.563	0.039
2	16.982	1.183
3	18.843	1.315
4	79.087	5.568
5	53.793	3.802
6	299.659	21.751

4.4 active power loss comparison, (from GERD to HOLETA 500/400 kV transmission line network)

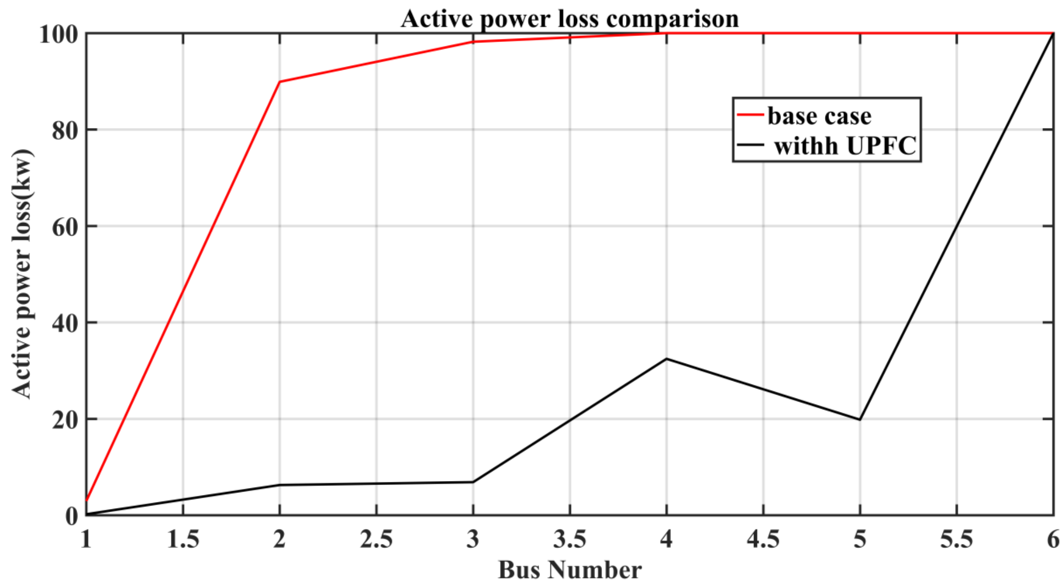

Figure4. 3 active power loss comparison, GERD to HOLETA 500/400 kV transmission line network

The Newton –Raphson Method sweep algorithm is used to assess the power flow in the GERD to HOLETA 500/400 kV transmission line network, with active power loss calculated for each bus. The last three buses experience the highest active power loss of 100 kW, as shown in Table 4.3. Additionally, the total active power loss for the network is 491.03 kW, as illustrated in the figure below. As shown in Table 4.3, following the integration of the UPFC into the GERD to HOLETA 500/400 kV transmission line network, the maximum active power loss of 100.00 kW occurs at the last bus. The total active power loss for the network is 165.5 kW. The active power losses for each bus in the network, with UPFC integration, are shown in Figure 4.3 below.

Active power in a system is the difference between the power injected into it and the power consumed by the connected loads. The Newton –Raphson Method load flow algorithm in MATLAB R2016a is used to calculate the active power loss in each branch. According to the simulation results, the total active power loss for the base case of the GERD to HOLETA 500/400 kV transmission line network is 491.03 kW. To maintain the stability of the transmission system, minimizing power loss is essential, and this can be significantly improved by using the UPFC to reduce current losses. The optimal size and placement of the UPFC were determined using the Grey Wolf Optimization (GWO) method, with the best configuration being

757.5 KVAR at bus 3. After installing the UPFC at the designated bus, the total active power loss reduced to 165.5 kW, a decrease from the original 491.03 kW.

Table4. 3 reactive power loss comparison

Bus no	Active Power Loss base case (without UPFC) (KW)	Active Power Loss with UPFC (KW)
1	2.932	0.203
2	89.889	6.262
3	98.208	6.852
4	100.000	32.436
5	100.000	198.076
6	100.000	100.000

4.5 voltage stability comparison

The voltage stability index is crucial when assessing voltage stability in power systems. It helps identify critical lines or buses within the network and evaluate the likelihood of a collapse. The MATLAB results for the base case of voltage stability in the GERD to HOLETA 500/400 kV transmission line network (without UPFC) are shown in Table 4.4. As indicated in Table 4.4 and Figure 4.4,below voltage stability ranges from a minimum of 0.521 pu to a maximum of 1.00 pu. The voltage stability index for each bus is presented in Figure 4.4 below . The ideal size and location of the UPFCs to be integrated into the network were determined using the Gray Wolf Optimization (GWO) method. The optimal average size of the UPFC was found to be 757.5 KVAR. The analysis of the final power flow with the UPFC installations showed an improvement in voltage stability (pu). The voltage stability values with UPFC integration are presented in Table 4.4. As shown in the table, voltage stability with the UPFC ranges from a minimum of 0.8530 pu to a maximum of 1.00 pu.

The voltage stability index (VSI) is an important measure for evaluating the stability of a power system's voltage profile. It indicates how close the system is to a point of voltage instability, which occurs when voltage levels drop significantly, potentially leading to equipment failures and widespread blackouts. The Newton –Raphson Method power flow analysis is used to calculate the VSI for both scenarios (with and without UPFC) in the GERD to HOLETA 500/400 kV transmission line network. According to the simulation results, the base-case bus voltage stability index for the GERD to HOLETA 500/400 kV transmission line network is 0.52

pu. Integrating the UPFC into the network at the optimal size and location improves system performance. As mentioned earlier, the Grey Wolf Optimization (GWO) method is essential for determining the placement and sizing of UPFCs in power transmission systems. After UPFC installation, the voltage stability improves, ranging from 0.85316 pu to 1.00 pu. In other words, the voltage stability index increases from 0.5214 pu to 0.85316 pu following UPFC integration. The voltage stability and performance comparisons for the GERD to HOLETA 500/400 kV transmission line network are shown in Table 4.4 and Figure 4.4 below, in both tabular and graphical formats.

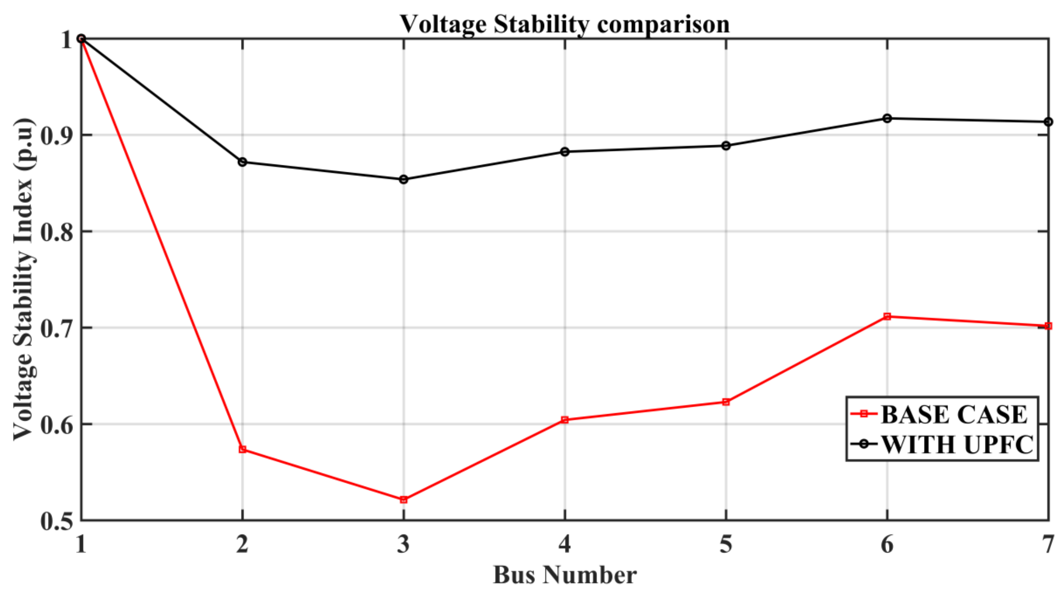

Figure4. 4 voltage stability index with comparison

Table4. 4 voltage stability comparison.

Bus no	Voltage stability index base case(without UPFC)	Voltage stability index with UPFC
1	1.000	1.000
2	0.573	0.871
3	0.521	0.853
4	0.604	0.882
5	0.623	0.888
6	0.711	0.917
7	0.7017	0.913

4.6 cost analysis

4.6.1 Cost benefit analysis of mitigation strategies

The expected annual financial losses caused by voltage sags can be significant. To minimize these losses, it is essential to install mitigation devices, such as the UPFC, while considering the associated costs. After installing the UPFC, power losses were reduced, which in turn led to a decrease in the financial losses caused by voltage sags [12]. Consequently, the financial losses associated with the use of UPFC are calculated below.

4.6.2 Economic Impact of Integrating UPFC

Integrating a (UPFC) can have several economic impacts on the power distribution system.

4.6.3 Energy losses (from GERD to HOLETA 500/400 kV transmission line network) before UPFC allocation

Annual energy loss of Holeta, substation (base case)

= P_{loss}*8760hrs

= 491.059 KW * 8760hrs

= 4301.598 MWhrs

Ethiopian Electric Utility tariff order for Industrial low voltage which is given in appendix C (EEU) at peak category rate/Eth Birr is 2.4050 birr/KWh

Cost of energy loss = E_{loss}*E.B

= 4301.598 MWhrs * 2.4050 birr/KWh

= 10,345,343.2 Eth birr

The results show that before installing UPFC the energy loss cost is 10.345 million Eth birr.

4.6.4 Energy losses of the (from GERD to HOLETA 500/400 kv transmission line network) after UPFC allocation

Annual energy loss of holeta substation

= $P_{loss\ reduction}$ *8760hrs

= 165.5 KW * 8760hrs

= 1449.78MWhrs

Cost of energy loss reduction = $E_{loss\ reduction}$*E.B

= 1449.8 MWhrs * 2.4050 birr/KWh

= 3,486,720 birr

The results show that before the installation of the UPFC, the energy loss cost was 10.345 million birr. However, after the UPFC was installed with the optimal size and placement in the GERD to HOLETA 500/400 kV transmission line network, the annual energy loss cost was reduced from 10.345 million birr to 3.486 million birr. This corresponds to a savings of 6.85 million birr in energy costs after UPFC compensation. The cost of UPFC per KVAR is $65, or 7800 birr (based on an exchange rate of 120 birr/$) [12]. Consequently, the total cost of a 757.5 KVAR UPFC is 5.708 million birr, including installation costs as detailed in [14].

- One unit of UPFC below 400Kvar size is 250,000 birr
- One unit of UPFC between 400KVAr-1500Kvar size is 1,000,000 birr
- One unit of UPFC above 1500KVAr size is 1,500,000 birr

Now the total cost for UPFC installation (Cost for equipment and installation cost will be 5.708 million Eth birr.

4.7 Methods of financial losses

The economic analysis uses standard financial measures, such as the Payback Period and Net Present Value (NPV) to assess the alternative [4].

4.7.1 Payback period

The Payback period is time required benefits required for an investment to recover its initial outlay. The payback time can be estimated by the following equation.

$$\text{Payback period (in months)} = \frac{Net\ Investment}{Net\ annual\ return} * 12$$

$$= \frac{Total\ cost}{\text{Energy loss reduction cost}} * 12$$

$$= \frac{\text{6.96 million birr}}{\text{6.5 million birr}} * 12$$

$$= \text{12months}$$

$$= 1\ year$$

CHAPTER FIVE

CONCLUSION, RECOMMENDATION FUTURE WORK

5.1. Summary

This chapter provides a detailed summary of the research findings related to the GERD to HOLETA 500/400 kV transmission line network. The aim of this chapter is to present the conclusions, recommendations, and suggestions for future work. In this thesis, the Grey Wolf Optimization (GWO) algorithm has been proposed for the optimal location and sizing of the UPFC in the network. Additionally, the Newton –Raphson load flow algorithm was developed to effectively incorporate the UPFC into the GERD to HOLETA 500/400 kV transmission line network, allowing for the evaluation of power loss, bus voltages, and the voltage stability index of the system.

5.2. Conclusion

This research aimed to improve power quality by enhancing the voltage profile and reducing losses. The optimization algorithm incorporates an objective function and a set of constraints. The Newton-Raphson load flow analysis was selected to compute all the required parameters for the existing system. The Newton-Raphson power flow analysis was performed for the base case and after the insertion of the UPFC. The results for the base case show that the minimum voltage magnitude and voltage stability index are 0.872 pu and 0.52 pu, respectively. All buses, except for bus 1, fall outside the voltage limits, indicating the need for an update. Active and reactive power losses in the base case are 491.02 kW and 468.9 KVAR, respectively. The maximum active power loss of 100 kW occurs at the last three buses. The GWO algorithm was used to determine the size and location of the reactive power-compensating device (UPFC), which aimed to reduce system power loss, improve the voltage profile, and enhance the voltage stability index. The effectiveness of this approach was demonstrated on the GERD to HOLETA 500/400 kV transmission line network. The required size of the compensating device, as determined by the GWO algorithm, is 757.5 KVAR. After placing the UPFC, another Newton –Raphson load flow analysis was conducted, resulting in improved voltage and stability, with values of 0.96598 pu and 0.85316 pu, respectively. Additionally, active power loss decreased to 165.5 kW, and reactive power loss reduced to 33.4 KVAR. The voltage profile of the network was significantly improved, remaining within the acceptable IEEE range, which aligns with Ethiopian standards.

The annual energy loss cost was reduced from 10.345 million birr to 3.486 million birr, and total cost of 757.5 KVAR UPFC including installation cost 5.708 million birr yielding a profit of 1.142 million birr, with the total cost covered within one year. In conclusion, this research successfully identifies the optimal size and placement of the UPFC for the GERD to HOLETA 500/400 kV transmission line network, leading to an overall improvement in system performance.

5.3 Recommendation

This thesis explores the impact of UPFC on the GERD to HOLETA 500/400 kV transmission line network, evaluating how it reduces power loss and enhances system performance. To improve the supply reliability of the GERD to HOLETA network, integrating UPFC is a more effective solution than constructing a new substation. I recommend that Ethiopian Electric Power (EEP) implement UPFC in the existing GERD to HOLETA 500/400 kV transmission line network to reduce power loss, improve power quality, and ensure a more stable and continuous power supply.

Reference

[1]. Jun Yong Liu, MPhil, Modelling and Control of Unified Power Flow Controller for Reinforcement of Transmission Systems, Brunel University, 1997.

[2]. Mohamed Jalboub, Investigation of the Application of UPFC Controllers for Weak Bus Systems Subjected to Fault Conditions, University of Bradford, 2012.

[3]. Sunil Kumar Jilledi, Implementing UPFC in the Power System Network to Control Power Flow and Minimization of Losses, American Journal of Energy and Power Engineering, 2015; 2(2): 12-19, January 2015.

[4]. Amir Kahyaei, Study of UPFC Location for Installing in Power System to Control Power Flow, Research Journal of Applied Sciences, Engineering, and Technology, 3(7): 640-649, 2011. ISSN: 2040-7467, July 25, 2011.

[5]. Naveen Singh and Piyush Agnihotri, Power System Stability Improvement Using FACTS Devices, International Journal of Advance Research and Development, Volume 3, Issue 4.

[6]. Azra Hasanovic, Modeling and Control of the Unified Power Flow Controller (UPFC), Morgantown, West Virginia, 2000.

[7]. Marcio Magalhães de Oliveira, Power Electronics for Mitigation of Voltage Sags and Improved Control of AC Power Systems, 2000.

[8]. Kalyan K. Sen, UPFC—Unified Power Flow Controller: Theory, Modeling, and Applications, Pittsburgh, PA 15235, USA, PE-282-PWRD-0-12-1997.

[9]. Djalel Dib, A. Rezaiguia, Z. Abada, Improving the Electric Power Quality by UPFC Systems in Electrical Networks, International Journal of Energy, Issue 4, Vol. 6, 2012.

[10]. Abebaw Yalew Mengistu, Study on Power Transfer Capability and Voltage Stability Improvement Using a Static VAR Compensator, May 2019.

[11]. Biniyam Abayneh, Study on Power Loss Reduction and Voltage Profile Improvement of the Kotebe Distribution System by Optimal Placement of D-STATCOM Using a Hybrid of Genetic Algorithm and Particle Swarm Optimization Method, Addis Ababa University, Ethiopia, April 2022.

[12]. Samson Ademola Adegoke & Yanxia Sun, Power System Optimization Approach to Mitigate Voltage Instability Issues, 27 Dec 2022.

[13]. S. K. Srivastava, S. N. Singh, and K. G. Upadhyay, FACTS Devices and their Controllers, National Power Systems Conference, NPSC 2002.

[14]. Fayez Kamel, K. El-Sayed, M. I. Elsayed, and Mokhtar H. Abdullah, Power Quality Improvement in Power Distribution Systems Using D-STATCOM, Vol. 4 No. 5, 2016. ISSN 2056-586.

[15]. Vijay Mohan Rachabattuni, Capacitor Banks and Their Effects on the Power System with High Harmonic Loads, April 2018.

[16]. Vaibhav S. Kale, Prashant R. Patil, and Ravi Khatri, Unified Power Flow Controller for Power Quality Improvement, ISSN: 2319–6378, Volume-1, Issue-10, August 2013.

[17]. B.T. Ramakrishna Rao, N. Gayatri, P. Balaji, and K. Sindhu, Modeling and Simulation of Static VAR Compensator Controller for Improvement of Voltage Level in Transmission Lines, Vol. 3, Issue 1, pp: (281-288), January - March 2015.

[18]. D. R. Patil & Komal K. Madhale, Design and Simulation Studies of D-STATCOM for Voltage Sag and Swell Mitigation, International Journal of Power System Operation and Energy Management, ISSN (PRINT): 2231 – 4407, Volume-2, Issue-1, 2012.

[19]. Vonjitina Fabien Randriambololona, Liva Graffin Rakotoarimanana, Eulalie Odilette Rafanjanirina, Minoson Rakotomalala, Zely Arivelo Randriamanantany, Influencing Factors on Power Losses in Electric Distribution Network, 20 May 2023.

[20]. V. K. Remya, P. Parthiban, V. Ansal, and B. Chitti Babu, Dynamic Voltage Restorer (DVR) – A Review, Journal of Green Engineering, Vol. 8, Issue 4, 519–572, River Publishers, 2018.

[21]. Ms. Frie Ayalew, Ms. Seada Hussen, Dr. Gopi Krishna Pasam, Optimization Techniques in Power System, International Journal of Engineering Applied Sciences and Technology, 2018.

[22]. Hyun-Jun Lee, Dae-Shik Lee, and Young-Doo Yoon, Unified Power Flow Controller Based on Autotransformer Structure, 13 December 2019.

[23]. Engr. M. Bilal, Engr. Dr. Ejaz Hassan, Engr. Hamza Zafar, Reactive Power Control in Power System Using Modified UPFC, Vol-4, Issue-7, July 2017.

[24]. Yasser Mohammed R. Alharbi, Application of Unified Power Flow Controller to Improve the Performance of Wind Energy Conversion System, March 2016.

[25]. Michael Lindgren, Modeling and Control of Voltage Source Converters Connected to the Grid, Technical Report No. 351, 1998.

[26]. Emmanuel Gbenga Dada, Stephen Bassi Joseph, David Opeoluwa Oyewola, Alaba Ayotunde Fadéle, Haruna Chiroma, Shafi'i Muhammad Abdulhamid, Application of Grey Wolf Optimization Algorithm: Recent Trends, Issues, and Possible Horizons, GU J Sci, 35(2): 485-504, 2022.

[27]. Vaibhav S. Kale, Prashant R. Patil, and Ravi Khatri, Unified Power Flow Controller for Power Quality Improvement, August 2013.

[28]. Salah, Mohd, Talpur, Noureen, and Talpur, Kashif, Adaptive Neuro-Fuzzy Inference System: Overview, Strengths, Limitations, and Solutions, 2017.

[29]. Joseph Sanam, Planning and Operation of DSTATCOM in Electrical Distribution Systems, National Institute of Technology Rourkela, India, June 2017.

[30]. Sreekanth Reddy Donapati and M.K. Verma, An Approach for Optimal Placement of UPFC to Enhance Voltage Stability Margin Under Contingencies, Fifteenth National Power Systems Conference (NPSC), IIT Bombay, December 2008.

[31]. G. Shahgholian, M. Mahdavian, M. Janghorbani, I. Eshaghpour, and E. Ganji, Analysis and Simulation of UPFC in Electrical Power Systems for Power Flow Control, Conference Paper, June 2017.

[32]. Ghazanfar Shahgholian and Mohammad Reza Yousefi, Performance Improvement of Electrical Power Systems Using UPFC Controller, Volume 5, Issue 3, 2019, pp. 5-13.

[33]. Yatharth Kumar Sharma and Vijay Mohan R, Capacitor Banks and Their Effect on Power Systems with High Harmonic Loads, India, April 6-8, 2018.

[34]. Worku Abera, Transmission Line Loss Minimization and Improvement of Voltage Profile Using Unified Power Flow Controller, Addis Ababa, Ethiopia, July 2019.

[35]. Tokuma Zeleke, Performance Evaluation of Transmission Lines for Power Loss Minimization and Voltage Profile Enhancement Using FACTS Devices, Addis Ababa, Ethiopia, January 2022.

Appendices

Appendix A

Network and equipment data

Table 500 kV transmission line conductor electrical data

No	Characteristics of conductor	explanation
1	Material of the conductor	Aluminum and steel
2	Actual area (total) in mm2	454.5
3	Standard overall diameter of conductor in mm	27.72
4	Resistance per km(ohm/km)	0.07173
5	Current carrying capacity	566 A at 65 deg. Centigrade,705 A at 75 deg. Centigrade

Table Data of 500/400 KV auto transformers

No	Type of transformer	Total capacity
1	500/400 kV(single phase types of capacity 250 MVA)	7*750 MVA=5250 MVA

Table Data of HOLETA 500/400 kV substation SVCs

No	Name of equipment	Capacity	Quantity
1	Static Var Compensator(SVC)	-450 to +450MVAr (total)	three
2	SVC transformer	400/33 kV, 315 MVA (each)	three

Table Data of Step up transformer at GERD

No of units(3 single phase transformers for each unit plus one spare)	3x(16+1)

Continuous rated power output	153 MVA
Nominal frequency	50 Hz
Rated power factor	0.9
Type	Single phase ,outdoor installation
Insulation type	Mineral oil
Cooling medium	Mineral oil
Cooling class	ONAN/ONAF
HV winding	500 kV
MV winding	18 kV
Winding connection	YNd11

Table Thyristor controlled reactor (TCR) data sheet (three in numbers) at HOLETA 500/400 kV substation.

Rated voltage	33 kV
Rated capacity	150 MVAr
Rated current	2624 A
Rated frequency	50 Hz

Table Data sheet of filter capacitor device (three for each TSC)

Rated voltage	33 kV
Rated capacity	50 MVAr
Rated current	875 A
Rated frequency	50 Hz
Tuning frequency	150 Hz

Table Data sheet of SVC transformer at HOLETA 500/400 kV substation (three in number)

Rated power	315 MVA
Rated voltage	400 ± 5%/33 kV
Type of cooling	ONAN/ONAF

Connection type	YNd11
Rated frequency	50 Hz
Number of phase	Three phase
Working condition	Outdoor

Table Data sheet of power transformer at HOLETA 500/400 kV substation (21 + 1 spare)

Rated power	250/250/25 MVA
Rated voltage	500/400/20 kV
Connection symbol	YNaOd11
Number of phase	Single –phase
Rated frequency	50 Hz
Working condition	outdoor
HV-MV impedance(impedance at rated frequency)	12.93%

Table GERD substation shunt Reactor datasheet

Designation	Technical parameter
Shunt reactor type	Oil immersed with conservator
Type of cooling	ONAN
Number of phases	Single phase
Rated frequency	50 Hz
Rated capacity	45MVAr X 3
Rated voltage	500/400 kV
Rated current	156 A
Rated reactance	1850.5 Ω
Winding connection	Star

Table DEDESA substation shunt Reactor datasheet

Description	Technical data
Installation	Outdoor
Rated Voltage	500/400 kV

Method of cooling	ONAN
Number of phases	3 phases
Frequency	50 Hz
Rated power for DEDESA substation on GERD line bay	135 MVAr
Rated power for DEDESA substation on Holeta line bay	135 MVAr
Rated power for DEDESA bus bar reactor	135 MVAr

Table HOLETA substation shunt Reactor datasheet

Description	Technical data
Installation	outdoor
Rated Voltage	500/400 kV
Method of cooling	ONAN
Number of phases	3 phases
Frequency	50 Hz
Rated power	90 MVAr

Algorithm program

```
function [bibc_matrix]=bibc_gen()
LINEDATA=linedata7;
%BUSDATA=busdata7;
baseKV=33;
baseMVA=2100;
PBASE=baseMVA*1000;
VBASE=(baseKV^2)/baseMVA;
%busdata_value=BUSDATA;
linedata_value=length(LINEDATA);
LINEDATA(:,4:5)=LINEDATA(:,4:5)/VBASE;
resistance_val=LINEDATA(:,4);
```

```
reactance_val=LINEDATA(:,5);
actual_imped=complex(resistance_val,reactance_val);
%busdata_value(:,2:3)= busdata_value(:,2:3)/PBASE);
imped_value=actual_imped;
bibc_matrix=zeros(linedata_value,linedata_value);
for i=1:linedata_value
    if LINEDATA(i,2)==1
        bibc_matrix(LINEDATA(i,3),LINEDATA(i,3))=1;
    else
        bibc_matrix(:,LINEDATA(i,3))=bibc_matrix(:,LINEDATA(i,2));
        bibc_matrix(LINEDATA(i,3),LINEDATA(i,3))=1;
    end
end
```

```
  function
[finalres_after_comp]=bold_flow_after(voltage_minimum,UPFC_place,data_pass_to_loadflow)
nbus=7;
voltage_minimum=V min;
voltage_maximum=V max;
capmaxsij_maximum=100;
distmaxij_maximum=10;
data_pass_to_loadflow{1}=voltage_minimum;
data_pass_to_loadflow{2}=voltage_maximum;
data_pass_to_loadflow{3}=capmaxsij_maximum;
data_pass_to_loadflow{4}=distmaxij_maximum;
source_num=[1];
[LINEDATA]=linedata7;
[BUSDATA]=busdata65(nbus);
```

```
baseKV=33;
baseMVA=100;
PBASE=baseMVA*10000;
VBASE=(baseKV^2)/baseMVA;
busdata_value=BUSDATA;
linedata_value=LINEDATA;
linedata_value(:,4:5)=linedata_value(:,4:5)/VBASE;
resistance_val=linedata_value(:,4);
reactance_val=linedata_value(:,5);
Distance=linedata_value(:,6);
actual_imped=complex(resistance_val,reactance_val);
busdata_value(:,2:3)=(busdata_value(:,2:3)/PBASE);
real_power= busdata_value(:,2);
imped_value=actual_imped;
[bibc_matrix]=bibc_gen();
bibc_matrix(source_num,:)=[];
bibc_matrix(:,source_num)=[];
final_bibc_matrix=bibc_matrix';
final_bcbv_matrix=final_bibc_matrix'*diag(actual_imped);
final_dlf_matrix=final_bcbv_matrix*final_bibc_matrix;
complex_load_d=complex(busdata_value(:,2),busdata_value(:,3));
% complex power load
complex_load_g=zeros(size(busdata_value,1),1);
UPFC_place=voltage_minimum;
loc_value=round(UPFC_place(1,:))
dsat_value=UPFC_place(1,:)
for ind=1:length(loc_value)
PG=0;
QG=(dsat_value(ind));
complex_load_g(loc_value(ind))=complex(PG/PBASE,QG/PBASE);
end
```

```
final_load_matrix=(complex_load_d-complex_load_g);
final_load_matrix(length(source_num))=[];
initial_volt_value=ones(size(busdata_value,1)-length(source_num),1);
% initial bus voltage
voltage_drop_value=initial_volt_value;
max_iter=300;
for ind_lop=1:max_iter
%newton –Raphson sweep
inject_current_data=conj(final_load_matrix./voltage_drop_value);
% injected current at each bus
IB=final_bibc_matrix*inject_current_data;
%get the cumulative injected current flowing through each branch
old_volt=voltage_drop_value;
volt_drop_each=final_dlf_matrix*inject_current_data;
%voltage drops along each branch.
voltage_drop_value=initial_volt_value-volt_drop_each;
old_volt1=(old_volt);
new_volt=(voltage_drop_value);
error_volt_tolr=max(abs(old_volt1-new_volt));
end
final_volt_data=[ones(length(source_num),1); voltage_drop_value];
rvolt=real(final_volt_data);
ivolt=imag(final_volt_data);
upfc =sum(double(length(find((rvolt<voltage_minimum) | (rvolt>voltage_maximum)))).^2);
locvoltm=find(rvolt>voltage_maximum);
rvolt(locvoltm)=voltage_maximum;
locvoltm=find(rvolt<voltage_minimum);
rvolt(locvoltm)=voltage_minimum;
final_volt_data=complex(rvolt,ivolt);
%h=abs(final_volt_data)
from_node=linedata_value(:,2);
```

```
to_node=linedata_value(:,3);
for ind=1:length(from_node) ;
   volt_diff_value(ind,:)=final_volt_data(from_node(ind))-final_volt_data(to_node(ind));
end
volt_diff_value1=abs(volt_diff_value);
%ploss=((volt_diff_value1.^2).*reactance_val)./(abs(imped_value).*abs( imped_value))*10^5;
ploss=abs(IB.^2).*(real(imped_value))*10^5;
% Each Line Loss in kWs
loc1=find(~(isnan(ploss)));
locp=find(ploss>capmaxsij_maximum);
ploss(locp)=capmaxsij_maximum;
loc3=find(~(isnan(Distance)));
Dist=find(Distance>distmaxij_maximum);
Distance(Dist)=distmaxij_maximum;
tot_distance=sum(Distance(loc3));
%<
%qloss=((volt_diff_value1.^2).*resistance_val)./(abs(imped_value).*abs(imped_value))*10^5;
qloss=(imag(imped_value)).*abs(IB.^2)*10^5;
% Each Line Loss in kVAr
loc2=find(~(isnan(qloss)));
power_loss=sum(ploss(loc1));
total_reactive_loss=sum(qloss(loc2));
finalvoltage=real(final_volt_data);
investment_cost=7445.89; %dollar/km
fixed_cost_rate=0.18; %fixed cost rate of feeder
Anual_investment_cost=investment_cost*fixed_cost_rate*tot_distance;
cost_loss=0.06;  %dollar/kwh;
Hours_in_year=8760;  % hrs
% energy_cost
load_location_factor=0.0465;
loss_loss=max(ploss);
```

```
loss_factor=loss_loss/power_loss;
%Anual_loss_energy_cost=power_loss*cost_loss*loss_factor*load_location_factor*Hours_in_y
ear;
generation_capability=11.976*1000; %out going feeder capacity
total_load=sum(real_power);
reserve_factor=generation_capability/(total_load*power_loss);
%cost_of_substation_cost=
f2=sum((1-finalvoltage).^2);
%% vsi calculation
for kk=1:length(busdata_value(:,2))
for ki=1:length(linedata_value(:,4))
vsival(kk)=(abs(finalvoltage(kk)).^4)-
4*(busdata_value(kk,2)*linedata_value(ki,4)+busdata_value(kk,3)*linedata_value(ki,5))*abs(fin
alvoltage(kk).^2)-
4*(busdata_value(kk,2)*linedata_value(ki,4)+busdata_value(kk,3)*linedata_value(ki,5)).^2;
end
end
loc3=find(~(isnan(vsival)));
f3=min(vsival);
w1=0.8;
w2=0.1;
w3=0.1;
%final_obj=w1*f1+w2*f2+w3\f3;
%finalres_after_comp{1}=final_obj;
finalres_after_comp{2}=power_loss;
finalres_after_comp{3}=finalvoltage;
finalres_after_comp{4}=vsival;
finalres_after_comp{5}=min(vsival);
finalres_after_comp{6}=total_reactive_loss;
finalres_after_comp{7}=finalvoltage;
finalres_after_comp{8}=min(finalvoltage);
```

```
finalres_after_comp{9}=max(finalvoltage);
finalres_after_comp{10}=max(vsival);
finalres_after_comp{11}=ploss;
finalres_after_comp{12}=qloss ;
voltage_profile_after_UPFC=finalres_after_comp{7};
min_voltage_profile_after_UPFC=finalres_after_comp{8}
max_voltage_profile_after_UPFC=finalres_after_comp{9}
voltage_stablity_index_after_UPFC=finalres_after_comp{4}
Active_power_loss_buses_WITH_UPFC=finalres_after_comp{11}
Reactive_power_loss_buses_WITH_UPFC=finalres_after_comp{12}
figure,plot(Active_power_loss_buses_WITH_UPFC,'k')
xlabel('Bus Number')
ylabel('Active power loss(Kw)')
title('Active power loss after UPFC')
grid on;
figure,plot(Reactive_power_loss_buses_WITH_UPFC,'k')
xlabel('Bus Number')
ylabel('Reactive power loss(VAR)')
title('Reactive power loss WITH_UPFC ')
grid on;
figure,plot(voltage_profile_after_UPFC,'rs-')
xlabel('Bus Number')
ylabel('Voltage (p.u)')
grid on;
title('Voltage Profile  After Compensation')
figure,plot(voltage_stablity_index_after_UPFC,'k-o')
xlabel('Bus Number');
ylabel('Voltage Stability Index (p.u)')
grid on;
title('Voltage Stability Index after  _UPFC')
```

```
% base case load follow
%clear all
%close all
function[finalres_base_case]=bold_flow_before(voltage_minimum,nbus,data_pass_to_loadflow)
[LINEDATA]=linedata7;
[BUSDATA]=busdata7;
nbus=7;
voltage_minimum=V min;
voltage_maximum=V max;
capmaxsij_maximum=100;
distmaxij_maximum=10;
data_pass_to_loadflow{1}=voltage_minimum;
data_pass_to_loadflow{2}=voltage_maximum;
data_pass_to_loadflow{3}=capmaxsij_maximum;
data_pass_to_loadflow{4}=distmaxij_maximum;
source_num=[1];
n=7;
baseKV=33;
baseMVA=2100;
PBASE=baseMVA*1000;
VBASE=(baseKV^2)/baseMVA;
busdata_value=(BUSDATA);
linedata_value=(LINEDATA);
linedata_value(:,4:5)=(linedata_value(:,4:5)/VBASE);
resistance_val=linedata_value(:,4);
reactance_val=linedata_value(:,5);
Distance=linedata_value(:,6);
actual_imped=complex(resistance_val,reactance_val);
busdata_value(:,2:3)=(busdata_value(:,2:3))/(PBASE);
real_power= busdata_value(:,2);
imped_value=actual_imped;
```

```
[bibc_matrix]=bibc_gen();
bibc_matrix(source_num,:)=[];
bibc_matrix(:,source_num)=[];
final_bibc_matrix=bibc_matrix';
final_bcbv_matrix=final_bibc_matrix'*diag(actual_imped);
final_dlf_matrix=final_bcbv_matrix*final_bibc_matrix;
complex_load_d=complex(busdata_value(:,2),busdata_value(:,3));
% complex power load
complex_load_g=zeros(size(busdata_value,1),1);
%Dsat_place;
%loc_value=round(Dsat_place(1));
%dsat_value=Dsat_place(2);
%for ind=1:length(loc_value)
PG=0;
%QG=(dsat_value(ind));
%complex_load_g(loc_value(ind))=complex(PG/PBASE,QG/PBASE);
%end
final_load_matrix=(complex_load_d-complex_load_g);
final_load_matrix(length(source_num))=[];
initial_volt_value=ones(size(busdata_value,1)-length(source_num),1);
% initial bus voltage
voltage_drop_value=initial_volt_value;
max_iter=300;
for ind_lop=1:max_iter
%newton Raphson sweep
inject_current_data=conj(final_load_matrix./voltage_drop_value);
% injected current at each bus
IB=final_bibc_matrix*inject_current_data;
%get the cumulative injected current flowing through each branch
old_volt=voltage_drop_value;
volt_drop_each=final_dlf_matrix*inject_current_data;
```

```
%voltage drops along each branch.
voltage_drop_value=initial_volt_value-volt_drop_each;
old_volt1=(old_volt);
new_volt=(voltage_drop_value);
error_volt_tolr=max(abs(old_volt1-new_volt));
end
final_volt_data=[ones(length(source_num),1); voltage_drop_value];
rvolt=real(final_volt_data);
ivolt=imag(final_volt_data);
Upfc=sum (double (length (find ((rvolt<voltage_minimum) | (rvolt>voltage_maximum)))). ^2);
Locvoltm=find (rvolt>voltage_maximum);
Rvolt (locvoltm)=voltage_maximum;
Locvoltm=find (rvolt<voltage_minimum);
Rvolt (locvoltm) =voltage_minimum;
final_volt_data=complex (rvolt, ivolt);
%h=abs (final_volt_data)
from_node=linedata_value (:,2);
to_node=linedata_value(:,3);
for ind=1:length(from_node) ;
   volt_diff_value(ind,:)=final_volt_data(from_node(ind))-final_volt_data(to_node(ind));
end
volt_diff_value1=abs(volt_diff_value);
%ploss=((volt_diff_value1.^2).*resistance_val)./(abs(imped_value).*abs( imped_value))*10^5;
ploss=abs(IB.^2).*(real(imped_value))*10^5;
%qloss=(imag(imped_value)).*abs(IB.^2)*10^5;
% Each Line Loss in kWs
loc1=find(~(isnan(ploss)));
locp=find(ploss>capmaxsij_maximum);
ploss(locp)=capmaxsij_maximum;
loc3=find(~(isnan(Distance)));
Dist=find(Distance>distmaxij_maximum);
```

```
Distance(Dist)=distmaxij_maximum;
tot_distance=sum(Distance(loc3));
%<
%qloss=((volt_diff_value1.^2).*reactance_val)./(abs(imped_value).*abs(imped_value))*10^5;
qloss=(imag(imped_value)).*abs(IB.^2)*10^5;
% Each Line Loss in kVAr
loc2=find(~(isnan(qloss)));
power_loss=sum(ploss(loc1));
total_reactive_loss=sum(qloss(loc2));
finalvoltage=real(final_volt_data);
investment_cost=7445.89; %dollar/km
fixed_cost_rate=0.18; %fixed cost rate of feeder
Anual_investment_cost=investment_cost*fixed_cost_rate*tot_distance;
cost_loss=0.06;  %dollar/kwh;
Hours_in_year=8760;  % hrs
% energy_cost
load_location_factor=0.0465;
loss_loss=max(ploss);
loss_factor=loss_loss/power_loss;
Anual_loss_energy_cost=power_loss*cost_loss*loss_factor*load_location_factor*Hours_in_yea
r;
generation_capability=11.976*1000; %out going feeder capacity
total_load=sum(real_power);
reserve_factor=generation_capability/(total_load*power_loss);
%cost_of_substation_cost=
%Annual_demand_cost=power_loss*load_location_factor*reserve_factor*(
%
total_annual_feeder_cost=Anual_investment_cost+Anual_loss_energy_cost+Annual_demand_c
ost;
f1=power_loss;
f2=sum((1-finalvoltage).^2);
```

```
%% vsi calculation
for kk=1:length(busdata_value(:,2))
for ki=1:length(linedata_value(:,4))
%vsival(kk)=(abs(finalvoltage(kk)).^4)-
(4*(busdata_value(kk,2)*linedata_value(ki,4)+busdata_value(kk,3)*linedata_value(ki,5)).^2)-
(4*(busdata_value(kk,2)*linedata_value(ki,5)-
busdata_value(kk,3)*linedata_value(ki,4)).^2)*abs(finalvoltage(kk).^2);
vsival(kk)=(abs(finalvoltage(kk)).^4)-
4*(busdata_value(kk,2)*linedata_value(ki,4)+busdata_value(kk,3)*linedata_value(ki,5))*abs(fin
alvoltage(kk).^2)-
4*(busdata_value(kk,2)*linedata_value(ki,4)+busdata_value(kk,3)*linedata_value(ki,5)).^2;
end
end
f3=min(vsival);
w1=0.8;
w2=0.1 ;
w3=0.1 ;
final_obj=w1*f1+w2*f2+w3\f3;
finalres_base_case{1}=final_obj;
finalres_base_case{2}=power_loss;
finalres_base_case{3}=finalvoltage
finalres_base_case{4}=vsival;
finalres_base_case{5}=min(vsival) ;
finalres_base_case{6}=total_reactive_loss;
finalres_base_case{7}=finalvoltage;
finalres_base_case{8}=min(finalvoltage) ;
finalres_base_case{9}=max(finalvoltage);
finalres_base_case{10}=max(vsival);
finalres_base_case{11}=ploss ;
finalres_base_case{12}=qloss ;
voltage_profile_base_case=finalres_base_case{7}
```

```
voltage_stablity_index_base_case=finalres_base_case{4}
Active_power_loss_buses_WITH_OUT_UPFC=finalres_base_case{11}
Reactive_power_loss_buses_WITH_OUT_UPFC=finalres_base_case {12}
legend('BASE CASE')
figure,plot(voltage_profile_base_case,'b-s')
xlabel('Bus Number')
ylabel('Voltage (p.u)')
title('Voltage Profile for base case ')
figure,plot(Reactive_power_loss_buses_WITH_OUT_UPFC,'r')
xlabel('Bus Number')
ylabel('Reactive power loss(VAR)')
title('Reactive power loss for base case')
figure,plot(Active_power_loss_buses_WITH_OUT_UPFC,'r')
xlabel('Bus Number')
ylabel('Active power loss(Kw)')
title('Active power loss for base case')
figure,plot(voltage_stablity_index_base_case,'r-s')
xlabel('Bus Number');
ylabel('Voltage Stability Index (p.u)')
grid on;
title('Voltage Stability Index for base case')
% this code returns intialy bus data of the system
function BUSDATA = busdata65(nbus)
% input data and variable initialization
  %        |Node|      |P(KW)|    |Q (KVAr)|
    BUSDATA=  [1.0000        0        0
               2.0000   10.4600   6.5400
               3.0000   99.8400   74.8190
               4.0000   13.9500   8.5000
               5.0000   13.9500   58.500
               6.0000   13.950    8.500
```

```
            7.0000   93.500    66.500  ];

busdata_value=(BUSDATA);
busdata_value(:,2:3)=(busdata_value(:,2:3));
real_power=busdata_value(:,2)*5.1;
reactive_power=busdata_value(:,3)*5.1;

tot=sum(real_power);
tot_tw=sum(reactive_power);
aparent=sqrt(tot^2+tot_tw^2);
 % this code returns intialy line data of the system
 % Any change in bus data such as load type P and Q can be edited here separetly;
 function LINEDATA= linedata46(nbus)
 % base case all load is of Pa type,
  %using smilar step brach data
   %            |br|     |f_n|   |to_n|    |R|      |X|      |D(km)|
       LINEDATA=[ 1.0000    1.0000    2.0000    1.2704    0.2438    3.2050
                  2.0000    2.0000    3.0000    0.3176    0.0600    0.8000
                  3.0000    3.0000    4.0000    0.2778    0.0533    0.7000
                  4.0000    4.0000    5.0000    0.7543    0.1295    1.9000
                  5.0000    5.0000    6.0000    0.3970    0.0762    1.0000
                  6.0000    6.0000    7.0000    0.9925    0.1905    2.5000];
linedata_value=(LINEDATA);
linedata_value(:,4:5)=(linedata_value(:,4:5));
resistance_val=linedata_value(:,4)*3.2;
reactance_val=linedata_value(:,5)*3.9;
% This function initialize the first population of search agents
function Positions=initialization(SearchAgents_no,dim,ub,lb)

lb=[1 100];
ub=[62 1200];
```

```
dim=2;
SearchAgents_no=100;
Boundary_no= size(ub,2); % numnber of boundaries

% If the boundaries of all variables are equal and user enter a signle
% number for both ub and lb
if Boundary_no==1
    Positions=rand(SearchAgents_no,dim).*(ub-lb)+lb;
end

% If each variable has a different lb and ub
if Boundary_no>1
    for i=1:dim
        ub_i=ub(i);
        lb_i=lb(i);
        Positions(:,i)=rand(SearchAgents_no,1).*(ub_i-lb_i)+lb_i;
    end
end



clear all
clc
nbus=7;
voltage_minimum=v min;
voltage_maximum=v max;
capmaxsij_maximum=100;
distmaxij_maximum=10.8;
QMIN_VALUE=120;
QMAX_VALUE=1200;
data_pass_to_loadflow{1}=voltage_minimum;
```

```
data_pass_to_loadflow{2}=voltage_maximum;
data_pass_to_loadflow{3}=capmaxsij_maximum;
data_pass_to_loadflow{4}=distmaxij_maximum;
N=100;
T=100;
%X=7;
UB=1200;
LB=100;
lb=1;
ub=7;
dim=2;
SearchAgents_no=300; % Number of search agents

Max_iteration=100; % Maximum numbef of iterations
[fobj]=Get_Functions_details();

[Best_score,Best_pos,GWO_cg_curve]=GWO(SearchAgents_no,Max_iteration,lb,ub,dim,fobj);
[finalres_base_case]=bold_flow_before(voltage_minimum,nbus,data_pass_to_loadflow);

display(['The best solution obtained by GWO is : ', num2str(Best_pos)]);
display(['The best optimal value of the objective funciton found by GWO is : ', num2str(Best_score)]);

finalresult_val=Best_pos(1:dim)
    UPFC_loc=round( finalresult_val(1))
    UPFC_SIZE=finalresult_val(2)
    UPFC_place=[UPFC_loc;UPFC_SIZE]


[finalres_after_comp]=bold_flow_after(voltage_minimum,UPFC_place,data_pass_to_loadflow)
  % display final result display('GWO RESULTS ');
```

```
POWER_LOSS_BASE_CASE=finalres_base_case{2}
VSI_MINIMUM_BASE_CASE=finalres_base_case{5}
Reactive_power_loss_base_case=finalres_base_case{6}
UPFC_LOCATION=UPFC_loc
UPFC_SIZE_kVAr=UPFC_SIZE
POWER_LOSS_WITH_UPFC=finalres_after_comp{2}
Reactive_power_loss_with_UPFC=finalres_after_comp{6}
VSI_MINIMUM_WITH_UPFC=finalres_after_comp{5}
Active_power_loss_percantage_reduction=(POWER_LOSS_BASE_CASE-
POWER_LOSS_WITH_UPFC)/(POWER_LOSS_BASE_CASE)*100;
Reactive_power_loss_percenatge_reduction=(Reactive_power_loss_base_case-
Reactive_power_loss_with_UPFC)/(Reactive_power_loss_base_case)*100;%
Minimum_voltage_base_case=finalres_base_case{8}
%Annual_loss_expense_base_case=finalres_base_case{13}
%Annual_loss_expense_after_UPFC=finalres_after_comp{13}
voltage_profile_base_case=finalres_base_case{7}
voltage_profile_after_UPFC=finalres_after_comp{7}
min_voltage_profile_after_UPFC=finalres_after_comp{8}
max_voltage_profile_after_UPFC=finalres_after_comp{9}
voltage_stablity_index_base_case=finalres_base_case{4}
voltage_stablity_index_after_UPFC=finalres_after_comp{4}
Active_power_loss_buses_WITH_OUT_UPFC=finalres_base_case{11}
Active_power_loss_buses_WITH_UPFC=finalres_after_comp{11}
Reactive_power_loss_buses_WITH_OUT_UPFC=finalres_base_case{12}
Reactive_power_loss_buses_WITH_UPFC =finalres_after_comp{12}
voltage_before_compensation=finalres_base_case{3}
voltage_stab_index_before_compensation=finalres_base_case{4}
voltage_after_compensation=finalres_after_comp{3}
voltage_stab_index_after_compensation=finalres_after_comp{4}

%figure,plot(voltage_before_compensation,'r')
```

```
%hold on,plot(voltage_after_compensation,'k')
%xlabel('Bus Number')
%ylabel('Voltage')
%grid on;
%legend('base case','with UPFC')
%title('Voltage Profile of the System Before and with UPFC')
%figure,plot(voltage_stab_index_with_UPFC,'r')
%hold on,plot(voltage_stab_index_with_UPFC,'k')
%xlabel('Bus Number')
%ylabel('Voltage Stability Index')
%grid on;
%legend('UPFC','BASE CASE')
%title('Voltage Stability Index for All Buses')
figure,plot(Active_power_loss_buses_WITH_OUT_UPFC,'r')
hold on,
plot(Active_power_loss_buses_WITH_UPFC,'k')
xlabel('Bus Number')
ylabel('Active power loss(Kw)')
title('Active power loss comparison')
grid on;
legend('base case',' withh UPFC')
figure,plot(Reactive_power_loss_buses_WITH_OUT_UPFC,'r')
hold on,
plot(Reactive_power_loss_buses_WITH_UPFC,'k')
xlabel('Bus Number')
ylabel('Reactive power loss(VAR)')
title('Reactive power loss comparison')
grid on;
legend('with  UPFC','base case')

legend('base case','with UPFC')
```

```
figure,plot(voltage_profile_base_case,'b-s')
hold on,
plot(voltage_profile_after_UPFC,'rs-')
xlabel('Bus Number')
ylabel('Voltage (p.u)')
grid on;
legend('BASE CASE','WITH UPFC')
title('Voltage Profile of the System without and with UPFC')
figure,plot(voltage_stablity_index_base_case,'r-s')
hold on,
plot(voltage_stablity_index_after_UPFC,'k-o')
xlabel('Bus Number');
ylabel('Voltage Stability Index (p.u)')
grid on;
legend('BASE CASE','WITH UPFC')
title('Voltage Stability Index for All Buses')
```